BANDWIDTH ENHANCEMENT OF DUAL PATCH MICROSTRIP ANTENNA ARRAY USING DUMMY EBG PATTERNS ON FEEDLINE

MANIK GUJRAL
B.Eng.(Hons.), NUS

A THESIS SUBMITTED

FOR THE DEGREE OF
MASTER OF ENGINEERING

DEPARTMENT OF ELECTRICAL AND COMPUTER ENGINEERING

NATIONAL UNIVERSITY OF SINGAPORE

2007

ACKNOWLEDGEMENTS

I would like to express my sincere gratitude to my project supervisors Prof. Li Le-Wei (ECE Department) and Dr. Liu Bo (DSI) for their guidance, patience and encouragement throughout the duration of this project.

In particular, I would like to thank Prof. Li for his continued support, help, encouragement and his useful suggestions throughout my M.Eng. degree candidature. Without his support, this thesis would not have been possible. I would also like to thank Prof. Ooi Ban Leong, Prof. Chen Xudong and Prof. Leong Mook Seng for their useful discussions during my candidature.

I would also like to thank Mr. Sing (Microwave Lab) and Mr. Jalil (PCB Fabrication Lab) and Mr. Jack Ng (Radar & Signal Processing Lab) for their help and assistance during the course of this project.

My gratitude is extended to my fellow laboratory members and many friends in RSPL and Microwave Lab for their help and advice when I encountered some difficulties in the project.

Last but not least, I take this opportunity to express my deepest thanks to my parents and my brother. Without their support, love and encouragement, it would not have been possible to pursue M.Eng. degree studies. I sincerely thank them.

TABLE OF CONTENTS

SUMMARY

Microstrip patch antennas have many advantages over conventional antennas which makes them suitable for a wide variety of applications. However, a major drawback of these antennas is the low bandwidth. Various techniques have been proposed by researchers to enhance its bandwidth.

In the recent years, electromagnetic bandgap (EBG) structures have attracted much attention in the microwave community for their unique properties. It has been shown that such structures help in improving the bandwidth of patch antennas.

In this thesis, we improve the bandwidth of a dual array patch antenna designed at 14.8 GHz by etching three different patterns that resemble conventional EBG structures on the feedline. The main purpose of the thesis is to have a percentage improvement in bandwidth of an EBG type antenna when compared to a reference antenna. We have termed these patterns as Dummy EBG patterns because these patterns are different from conventional EBG structures but resemble in certain properties and functions to them. These dummy EBG patterns are small and compact in size. It has been shown that a considerable improvement in bandwidth can be achieved.

Also, we have shown that position of the feedline plays a significant role in bandwidth enhancement. It is shown that to get a good improvement in bandwidth, the dummy EBG pattern feedline should be placed at an appropriate position closer to the lower edge of the patch antenna.

LIST OF TABLES

LIST OF FIGURES

LIST OF SYMBOLS

λ	Wavelength
ε_r	Dielectric constant
ε_{reff}	Effective dielectric constant
h	Height of dielectric substrate
W	Width of patch
c	Speed of light
Γ	Reflection coefficient
Z	Input impedance
Z_0	Characteristic impedance
δ_{eff}	Effective loss tangent
Q_T	Total antenna quality factor
Q_d	Quality factor of dielectric
ω_r	Angular resonant frequency
W_T	Total energy stored in patch at resonance
P_d	Dielectric loss
$\tan\delta$	Loss tangent of dielectric
Q_c	Quality factor for radiation
P_c	conductor loss
Δ	Skin depth of conductor

P_r	Power radiated from patch
F(g)	Function of g
a_n	Unknown constant
g_n	Basis or expansion function
w_1	Weighting functions
$\underline{E}$	Incident electric field
$\underline{J}$	Induced current
f_e	Linear operator
b_i	i^{th} basis function
d	Spacing between elements
M	Total number of elements

CHAPTER 1

INTRODUCTION

1.1 A Brief Introduction

Microstrip patch antennas are the most common form of printed antennas. They are popular for their low profile geometry, light weight and low cost. These antennas have many advantages when compared to conventional antennas and hence have been used in a wide variety of applications ranging from mobile communication to satellite, aircraft and other applications [1].

Similarly, electromagnetic bandgap (EBG) structures have attracted much attention in the recent years in the microwave community for its unique properties. These structures are periodic in nature that forbids the propagation of all electromagnetic surface waves within a particular frequency band – called the bandgap – thus permitting additional control of the behavior of electromagnetic waves other than conventional guiding and/or filtering structures. Various compact structures have been proposed and studied on antenna systems. Radiation efficiency and directivity of antennas have been improved using such structures [2]-[3].

1.2 Problem to be Solved : Low Bandwidth of Patch Antenna

In spite of the many advantages that patch antennas have in comparison to conventional antennas, they suffer from certain disadvantages. The major drawback of such antennas is the narrow bandwidth [1].

In this thesis, the narrow bandwidth problem of a patch antenna is tackled and solved. A dual array patch antenna is used as a reference antenna and efforts are made to improve its bandwidth by etching the feedline connecting the two patches using EBG type patterns. Three different EBG patterns are introduced in the thesis and measurement results confirm a considerable improvement in bandwidth. Also, significance of the position of feedline connecting the twin patches with respect to the bandwidth is studied.

1.3 Review of Past Work: Approaches to Enhance Bandwidth

Various efforts have been made by researchers all over the world to improve the bandwidth of a patch antenna. Some of the different techniques are mentioned in this section.

One way to increase the bandwidth is to either increase the height of the dielectric or decrease the dielectric constant. However, the first approach would make it unsuitable for low profile structures while the latter approach will make the matching circuit to the patch impractical due to excessively wide lines. Equation (1.1) shows the relationship of bandwidth to wavelength (λ), height of the dielectric (t), and dielectric constant (ε_r); while the equation for wavelength is given in Equation (1.2) where c is the wavelength and f is the center frequency, as follows:

$$B = 3.77\left(\frac{\varepsilon_r - 1}{\varepsilon_r^2}\right)\frac{t}{\lambda}, \tag{1.1}$$

$$\lambda = \frac{c}{f}. \tag{1.2}$$

The bandwidth equation is valid for $t/\lambda << 1$. The bandwidth is defined as the fractional bandwidth relative to the center frequency for a VSWR less than 2:1. VSWR stands for voltage standing wave ratio, shown in Equation (1.3), and is measured according to the reflection coefficient (Γ) of the input feeding network:

$$VSWR = \frac{1+|\Gamma|}{1-|\Gamma|}. \tag{1.3}$$

The reflection coefficient is found from the input impedance, Z, into the patch and is shown in Equation (1.4), where Z_0 is the characteristic impedance and is usually 50Ω.

$$\Gamma = \frac{Z - Z_o}{Z + Z_o}. \tag{1.4}$$

A VSWR of 2:1 implies a reflection coefficient of approximately -10dB.

The use of U slot and L probe in the design of small size microstrip antennas has been considered by Shakelford *et al.* [4]. Different designs have been proposed by these authors who utilized various size reduction techniques: utilizing a microwave substrate material, the addition of a shorting wall, and the addition of a shorting pin. A considerable improvement in bandwidth is observed in all the designs.

Another method employed by researchers is using compound techniques [5]. These techniques include adjusting the displacement of patches, setting two pairs conducting bars around the lower patch as parasitic radiator and loading a capacitive disk on the top of probe. A new type of stacked microstrip patch antenna is studied using these compound techniques and the frequency bandwidth has been remarkably improved.

In [6], the bandwidth of an aperture coupled microstrip patch antenna has been studied and improved by using an appropriate impedance matching network using filter design techniques. The initial useful antenna characteristics were maintained for the proposed new feed configuration.

The use of two triangular structures for microstrip patch antennas to improve the bandwidth has also been studied [7]. In it, two separate triangular patches are used to form patch antenna with a small spacing left between the two triangular patches. A full-wave spatial-domain technique together with the closed-form Green's function is employed for obtaining the S-parameters of microstrip antennas and measurement results confirm a considerable improvement in bandwidth.

The use of unbalanced structures in the design of patch antenna to improve VSWR characteristic has also been studied previously [8]. Similar to [7], a full wave spatial domain MoM together with the closed-form Green functions have been employed for characterizing high-frequency S-parameters of microstrip discontinuities. The obtained numerical results are compared with existing measurement data which show a good agreement to each other. Also, improvement in bandwidth is observed in the design.

Another technique that has been employed recently to improve the bandwidth of patch antennas is using electromagnetic bandgap (EBG) structures [2]. Different shapes and sizes of EBG structures such as mushroom EBG structure and spiral EBG structure have been proposed and studied and has led to considerable improvement in bandwidth of patch antennas.

In this thesis, we will study a dual array patch antenna operating at a high frequency and etch different EBG patterns on the feedline to improve the bandwidth.

1.4 Original Contributions

We propose three different types of dummy EBG patterns that are etched effectively on the feedline connecting the two patches of a dual array patch antenna. These dummy EBG patterns are compact and small in size. These patterns resemble conventional EBG structures in certain properties and functions and hence have been termed as dummy EBG patterns. A considerable improvement in bandwidth is observed in antennas having dummy EBG patterns on feedline. Hence, we are able to improve the low bandwidth problem of a patch antenna.

Also, we find that feedline connecting the two patches of the antenna plays a significant role in the bandwidth. When the position of the feedline is closer to the lower edge of the twin patches, we observe that a greater improvement in bandwidth is obtained for antenna having EBG patterns etched on feedline when compared to a reference antenna having no EBG patterns on the feedline.

1.5 List of Publications

1. **Manik Gujral**, Tao Yuan, Cheng-Wei Qiu, Le-Wei Li, and Ken Takei, "Bandwidth Increment of Microstrip Patch Antenna Array with Opposite Double-E EBG Structure for Different Feed Positions", Proceedings of the 11th International Symposium on Antennas and Propagation, November 1-4 2006, Singapore.

2. **Manik Gujral**, Tao Yuan, Le-Wei Li, and Cheng-Wei Qiu, "Bandwidth Improvement of Microstrip Patch Antenna Array Performance Using Different EBG Structures on the Feedlines", (International Invited Paper), Proceedings of the 6th Asia-Pacific Engineering Research Forum on Microwave and Electromagnetic Theory, pp.16-24, August 20-21 2006, Shanghai, China.

3. **Manik Gujral**, Tao Yuan, Cheng-Wei Qiu, and Le-Wei Li, "Bandwidth Improvement of Microstrip Patch Antenna Array by Etching Dummy EBG Pattern on Feedline" (Submitted to and under review by IEICE Transactions on Communications).

4. **Manik Gujral**, Tao Yuan, Le-Wei Li, and Cheng-Wei Qiu, "Some Dummy EBG Patterns for Bandwidth Improvement of Dual Array Patch Antenna" (Submitted to and under review by IEEE Transactions on Antennas and Propagation).

1.6 Organization of Thesis

The thesis is divided into 5 chapters. Chapter 1 includes a brief introduction to patch antennas and electromagnetic bandgap (EBG) structures together with the problem to be solved. Past work by researchers from all over the world has been put forth. Original contributions and resultant publications arising from this research are also highlighted in this chapter.

Chapter 2 provides the literature review and the theory involved in the research work. Theory on patch antenna includes its advantages and disadvantages. Various feeding techniques and methods of analysis of patch antennas are mentioned in this chapter. Also, a brief introduction to array analysis is made. Next, theory on EBG structures has been briefed together with its various applications. Finally, a brief introduction to the CAD software used is mentioned.

Chapter 3 provides an in-depth design procedure for different antenna structures and dummy EBG patterns. The prototype or the reference antenna and the design of its three variants (antenna variant-1, antenna variant-2 and antenna variant-3) are mentioned in this chapter. The fabricated antennas are also shown in this chapter.

Chapters 4 includes a comparison of results between reference antenna and its three variants, namely, antenna variant-1, antenna variant-2 and antenna variant-3. Simulation and Measurement results have been mentioned. The effect of changing positions of the feedline on the bandwidth is also shown by taking out different simulation results.

Chapter 5 summarizes all the important observations and results from previous chapters. Potential future work is also put forth.

CHAPTER 2

FUNDAMENTAL THEORY

2.1 Introduction

In this chapter, a detailed theory on microstrip patch antennas and electromagnetic bandgap (EBG) structure is given. Sections 2.2 to 2.4 cover theory on patch antennas, feeding techniques and different methods for analysis of patch antennas. This is followed by theory on antenna arrays in Section 2.5. Section 2.6 gives a description about EBG structures and their applications. Finally, a brief introduction to CAD software used for simulations is mentioned in Section 2.7.

2.2 Microstrip Patch Antennas

Microstrip patch antennas are the most common form of printed antennas. They are popular for their low profile, geometry and low cost.

A microstrip device in its simplest form is a layered structure with two parallel conductors separated by a thin dielectric substrate. The lower conductor acts as a ground plane. The device becomes a radiating microstrip antenna when the upper conductor is a patch with a length that is an appreciable fraction of a wavelength (λ), approximately half a wavelength ($\lambda/2$). In other words, a microstrip patch antenna consists of a radiating patch on one side of a dielectric substrate which has a ground plane on the other side as shown in Fig. 2.1.

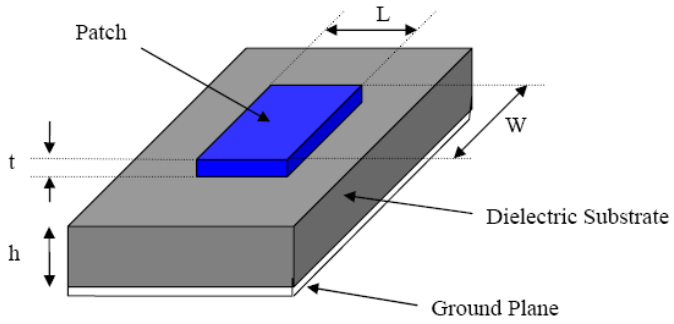

Fig. 2.1 Typical microstrip patch antenna [1]

The patch is generally made of conducting material such as copper or gold and can take any possible shape. Some of the typical patch shapes are shown in Fig. 2.2.

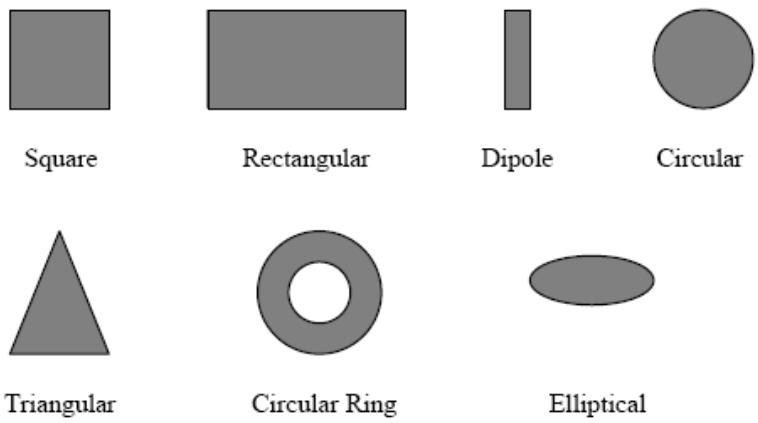

Fig. 2.2 Different shapes and sizes of patch [1]

The radiating patch and the feed lines are usually photo etched on the dielectric substrate. Microstrip patch antennas radiate primarily because of the fringing fields between the patch edge and the ground plane.

Microstrip patch antennas have many advantages when compared to conventional antennas. As such, they have found usage in a wide variety of applications ranging from embedded antennas such as in a cellular phone, pagers etc. to telemetry and

communication antennas on missiles and in satellite communications. Some of their principal advantages discussed by [1] and Kumar and Ray [9] are:

- Light weight and low volume
- Low profile planar configuration which can be easily made conformal to host surface
- Low fabrication cost, hence can be manufactured in large quantities
- Supports both, linear as well as circular polarization
- Can be easily integrated with microwave integrated circuits (MICs)
- Capable of dual and triple frequency operations
- Mechanically robust when mounted on rigid surfaces.

In spite of the many advantages, these antennas also suffer from a number of disadvantages. Some of them have been discussed by Kumar and Ray in [9] and Garg *et al.* in [10] and they are given below:

- Narrow bandwidth
- Low efficiency
- Low gain
- Extraneous radiation from feeds and junctions
- Poor end fire radiator except tapered slot antennas
- Low power handling capacity
- Surface wave excitation.

Microstrip patch antennas have a very high antenna quality factor (Q). Q represents the losses associated with the antenna. Typically there are radiations, conduction (ohmic), dielectric and surface wave losses. For very thin substrates, the losses due to

surface waves are very small and can be neglected. However, as the thickness increases, an increasing fraction of the total power delivered by the source goes into a surface wave. This surface wave contribution is considered as an unwanted power loss since it is ultimately scattered at the dielectric bends and causes degradation of the antenna characteristics. The surface waves can be minimized by use of photonic bandgap structures as discussed by Qian *et al*. [11]. Other problems such as lower gain and lower power handling capacity can be overcome by using an array configuration for the elements.

2.3 Feed Techniques for Patch Antennas

Microstrip antennas are fed by a variety of methods that are broadly classified into two main categories, namely, contacting and non-contacting. In the contacting method, the RF power is fed directly to the radiating patch using a connecting element such as a microstrip line. In the non-contacting method, electromagnetic field coupling is done to transfer power between the microstrip line and the radiating patch [1].

The four most popular feed techniques used are the microstrip line, coaxial probe (both contacting schemes), aperture coupling and proximity coupling (both non-contacting schemes). These are discussed in subsequent sections.

2.3.1 Microstrip Line Feed

In this type of feed technique, a conducting strip is connected directly to the edge of the microstrip patch as shown in Fig. 2.3. This strip is smaller in width as compared to the patch. The major advantage of this arrangement is that the feed can be etched on the same substrate to provide a planar structure.

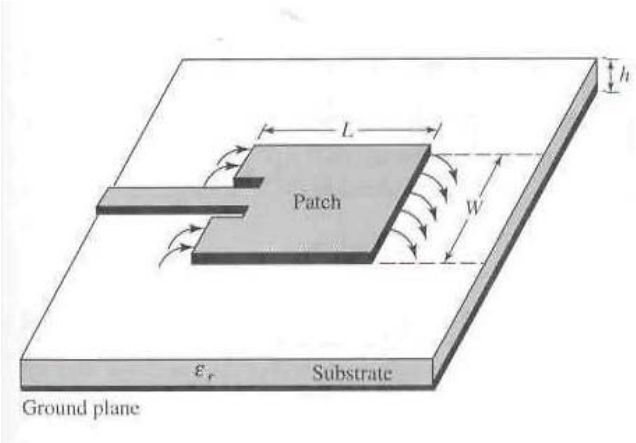

Fig. 2.3 Microstrip line feed for patch antenna [1]

In many cases, an inset cut feed is preferred over edge feed. The purpose of the inset cut in the patch is to match the impedance of the feed line to the patch without the need for any additional matching element. It is an easy feeding technique that is easy to fabricate and provides simplicity in modeling as well as impedance matching. However as the thickness of the dielectric substrate being used increases, surface waves and spurious feed radiation also increases, which hampers the bandwidth of the antenna [1]. The feedline radiation also leads to undesired cross polarized radiation.

2.3.2 Coaxial Feed

The coaxial feed or probe feed is a very common contacting scheme of feeding patch antennas. The configuration of a coaxial feed is shown in Fig. 2.4. As seen from Fig. 2.4, the inner conductor of the coaxial connector extends through the dielectric and is soldered to the radiating patch, while the outer conductor is connected to the ground plane.

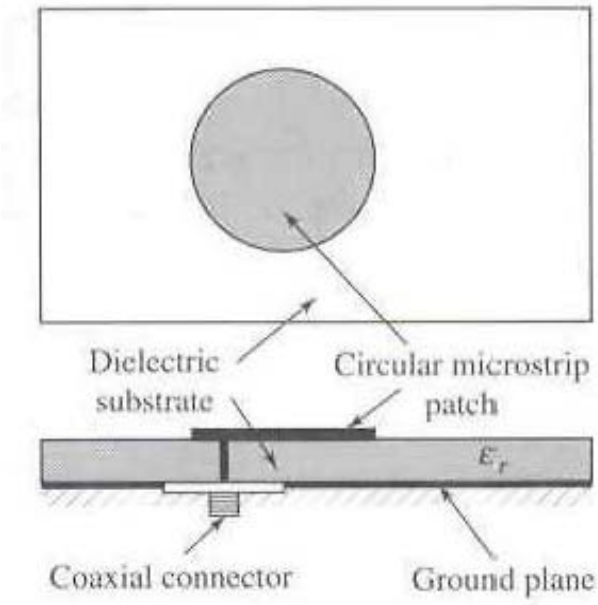

Fig. 2.4 Coaxial feed for patch antenna [1]

The main advantage of this type of feeding scheme is that the feed can be placed at any desired location inside the patch in order to match with its input impedance. This feed method is easy to fabricate and has low spurious radiation.

However, its major disadvantage is that it provides narrow bandwidth and is difficult to model since a hole has to be drilled in the substrate and the connector protrudes outside the ground plane, thus not making it completely planar for thick substrates ($h > 0.02\lambda_0$). Also, for thicker substrates, the increased probe length makes the input impedance more inductive, leading to matching problems [9]. It is seen as above that for a thick dielectric substrate, which provides broad bandwidth, the microstrip line feed and the coaxial feed suffer from numerous disadvantages. The non-contacting feed techniques which have been discussed below, solve these problems.

2.3.3 Aperture Coupled Feed

In this type of feed technique, the radiating patch and the microstrip feed line are separated by the ground plane as shown in Fig 2.5. Coupling between the patch and the feed line is made through a slot or an aperture in the ground plane.

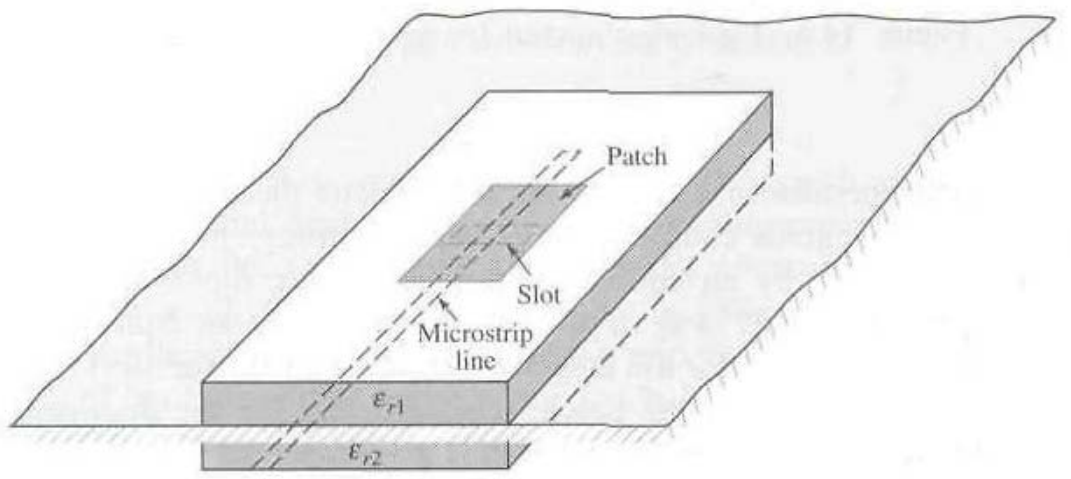

Fig. 2.5 Aperture coupled feed for patch antenna [1]

The coupling aperture is usually centered under the patch, leading to lower cross-polarization due to symmetry of the configuration. The amount of coupling from the feed line to the patch is determined by the shape, size and location of the aperture. Since the ground plane separates the patch and the feed line, spurious radiation is minimized. Generally, a high dielectric material is used for the bottom substrate and a thick, low dielectric constant material is used for the top substrate to optimize radiation from the patch [1].

The major disadvantage of this feed technique is that it is difficult to fabricate due to multiple layers, which also increases the antenna thickness. This feeding scheme also provides narrow bandwidth.

2.3.4 Proximity Coupled Feed

This type of feed technique is also called the electromagnetic coupling scheme. As shown in Fig. 2.6, two dielectric substrates are used such that the feed line is between the two substrates and the radiating patch is on top of the upper substrate.

The main advantage of this feed technique is that it eliminates spurious feed radiation and provides higher bandwidth in comparison to the other feeding techniques (as high as 13%) [1], due to overall increase in the thickness of the microstrip patch antenna. This scheme also provides choices between two different dielectric media, one for the patch and one for the feed line to optimize the individual performances.

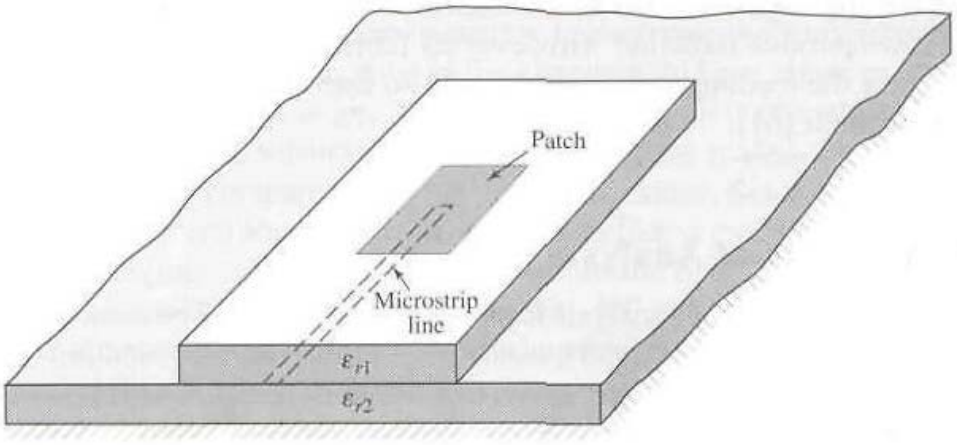

Fig. 2.6 Proximity coupled feed for patch antenna [1]

Matching can be achieved by controlling the length of the feed line and the width-to-line ratio of the patch. The major disadvantage of this feed scheme is that it is difficult to fabricate because of the two dielectric layers which need proper alignment. Also, there is an increase in the overall thickness of the antenna.

Fig 2.7 shows the equivalent circuits of the four types of feed techniques [1] while Table 2.1 summarizes the characteristics of the different feed techniques of patch antennas.

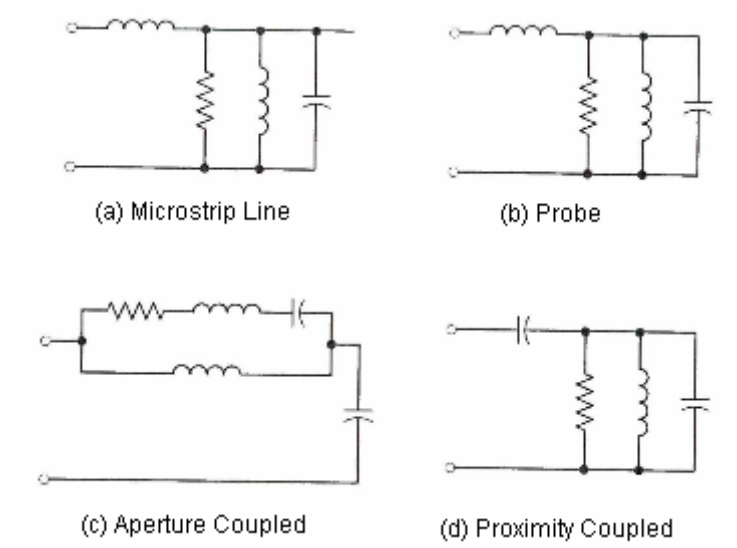

Fig. 2.7 Equivalent circuits for different feed techniques for patch antennas [1]

Table 2.1 Comparison between different feed techniques for patch antennas [12]

Characteristics	**Microstrip Line Feed**	**Coaxial Feed**	**Aperture Coupled Feed**	**Proximity Coupled Feed**
Spurious feed radiation	More	More	Less	Minimum
Reliability	Better	Poor due to soldering	Good	Good
Ease of fabrication	Easy	Soldering and drilling required	Alignment required	Alignment required
Impedance matching	Easy	Easy	Easy	Easy
Bandwidth (achieved with impedance matching)	2-5%	2-5%	2-5%	13%

2.4 Methods of Analysis for Patch Antennas [1]

The most popular models for analysis of microstrip patch antennas are the transmission line model, cavity model, and full wave model [1] (which include primarily integral equations / moment method).

The transmission line model is the simplest of all and it gives good physical insight but it is less accurate. The cavity model is more accurate and gives good physical insight but is complex in nature. The full wave models are extremely accurate, versatile and can treat single elements, finite and infinite arrays, stacked elements, arbitrary shaped elements and coupling. These give less insight as compared to the two models mentioned above and are far more complex in nature.

2.4.1 Transmission Line Model

This model represents the microstrip antenna by two slots of width W and height h, separated by a transmission line of length L. The microstrip is essentially a non-homogeneous line of two dielectrics, typically the substrate and air. A typical microstrip line is shown in Fig. 2.8 while the electric field lines associated with it are shown in Fig. 2.9.

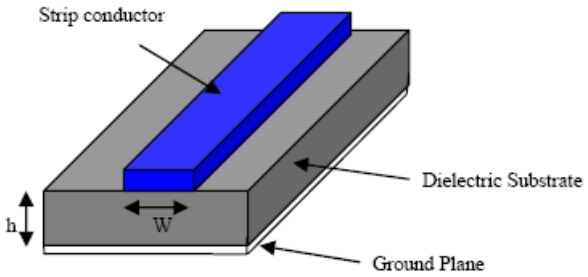

Fig. 2.8 Microstrip line [1]

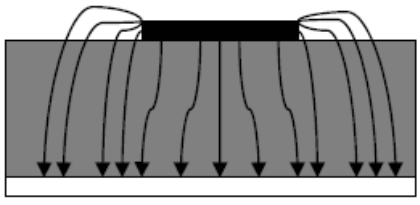

Fig. 2.9 Electric field lines [1]

[1] M.Sc. Thesis, "Design of a compact microstrip patch antenna for use in Wireless/Cellular Devices, pp. 38-47, The Florida State University, 2004.

As seen from Fig. 2.9, most of the electric field lines reside in the substrate while some electric field lines exist in the air. As a result, this transmission line cannot support pure transverse-electric-magnetic (TEM) mode of transmission since the phase velocities would be different in the air and the substrate. Instead, the dominant mode of propagation would be the quasi-TEM mode. Hence, an effective dielectric constant (ε_{reff}) must be obtained in order to account for the fringing and the wave propagation in the line.

The value of ε_{reff} is slightly less than ε_r, because the fringing fields around the periphery of the patch are not confined in the dielectric substrate but are also spread in the air as shown in Fig. 2.9 above. The expression for ε_{reff} is given by Balanis [13] as:

$$\varepsilon_{reff} = \frac{\varepsilon_r + 1}{2} + \frac{\varepsilon_r - 1}{2}\left[1 + 12\frac{h}{W}\right]^{-\frac{1}{2}} \tag{2.1}$$

where ε_{reff} denotes effective dielectric constant, ε_r stands for dielectric constant of substrate, h represents height of dielectric substrate, and W identifies width of the patch.

Figure 2.10 shows the transmission line model for patch antenna, where Fig. 2.10(a) is the patch antenna, Fig. 2.10(b) is the top view and Fig. 2.10(c) is the side view of the antenna.

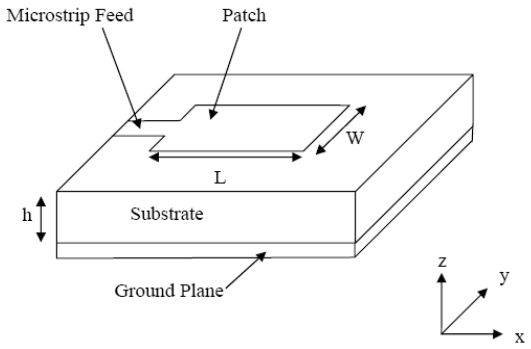

(a) Microstrip patch antenna

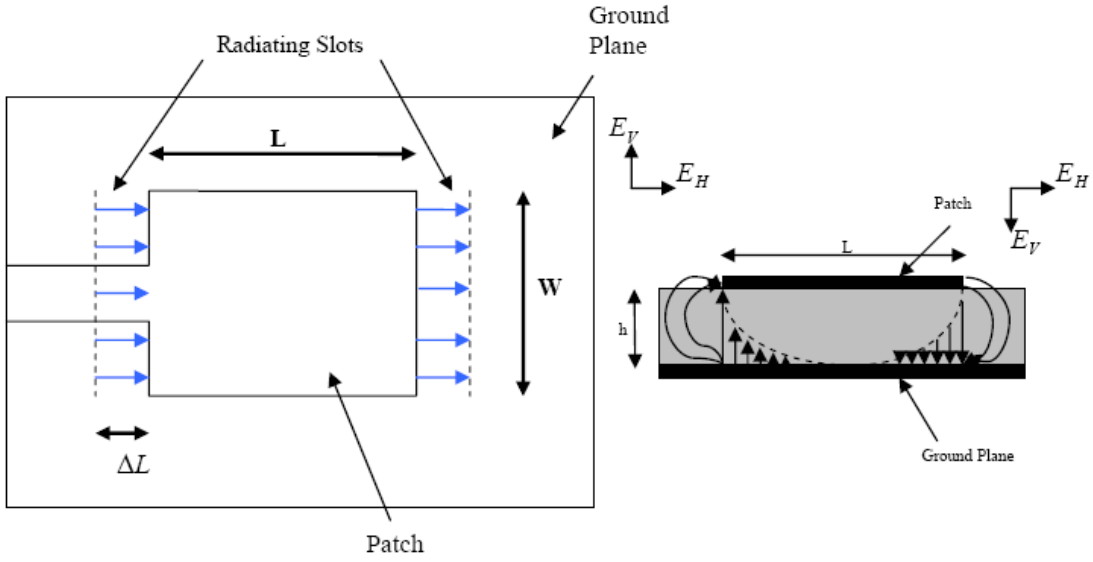

(b) Top view of antenna (c) Side view of antenna

Fig. 2.10 Transmission line model for patch antenna [1]

In order to operate in the fundamental TM_{10} mode, the length of the patch must be slightly less than $\lambda/2$, where λ is the wavelength in the dielectric medium and is equal to $\lambda_0/\sqrt{\varepsilon_{reff}}$, where λ_0 is the free space wavelength. The TM_{10} model implies that the field varies one $\lambda/2$ cycle along the length and there is no variation along the width of the patch. In Fig. 2.10(b) shown above, the microstrip patch antenna is

represented by two slots, separated by a transmission line of length L and open circuited at both the ends. Along the width of the patch, the voltage is maximum and current is minimum due to the open ends. The fields at the edges can be resolved into normal and tangential components with respect to the ground plane.

It is seen from Fig 2.10(c) that the normal components of the electric field at the two edges along the width are in opposite directions and thus out of phase since the patch is $\lambda/2$ long and hence they cancel each other in the broadside direction. The tangential components (seen in Fig 2.10(c)), which are in phase, means that the resulting fields combine to give maximum radiated field normal to the surface of the structure.

Hence the edges along the width can be represented as two radiating slots, which are $\lambda/2$ apart and excited in phase and radiating in the half space above the ground plane. The fringing fields along the width can be modeled as radiating slots and electrically the patch of the microstrip antenna looks greater than its physical dimensions. The dimensions of the patch along its length have now been extended on each end by a distance ΔL, which is given empirically by Hammerstad [14] as

$$\Delta L = 0.412h\frac{\left(\varepsilon_{reff}+0.3\right)\left(\frac{W}{h}+0.264\right)}{\left(\varepsilon_{reff}-0.258\right)\left(\frac{W}{h}+0.8\right)}. \tag{2.2}$$

The effective length of the patch L_{eff} now becomes

$$L_{eff} = L + 2\Delta L . \tag{2.3}$$

For a given resonance frequency f_0, the effective length is given by [9] as

$$L_{eff} = \frac{c}{2 f_0 \sqrt{\varepsilon_{reff}}} . \tag{2.4}$$

For a rectangular microstrip patch antenna, the resonance frequency for any TM_{nm} mode is given by James and Hall [15] as

$$f_0 = \frac{c}{2\sqrt{\varepsilon_{reff}}} \left[\left(\frac{m}{L} \right)^2 + \left(\frac{n}{W} \right)^2 \right]^{\frac{1}{2}} \tag{2.5}$$

where m and n are modes along L and W, respectively.

For efficient radiation, the width W is given by Bahl and Bhartia [16] as

$$W = \frac{c}{2 f_0 \sqrt{\frac{(\varepsilon_r + 1)}{2}}} . \tag{2.6}$$

2.4.2 Cavity Model

Although the transmission line model discussed in the previous section is easy to use, it has some inherent disadvantages. Specifically, it is useful for patches of rectangular design and it ignores field variations along the radiating edges. These disadvantages can be overcome by using the cavity model. A brief overview of this model is given below.

In this model, the interior region of the dielectric substrate is modeled as a cavity bounded by electric walls on the top and bottom. The basis of this assumption is the following observations for thin substrates ($h << \lambda$) [10]:

- Since the substrate is thin, the fields in the interior region do not vary much in the z direction, i.e. normal to the patch.
- The electric field is z directed only, and the magnetic field has only the transverse components H_x and H_y in the region bounded by the patch metallization and the ground plane. This observation provides for the electric walls at the top and the bottom.

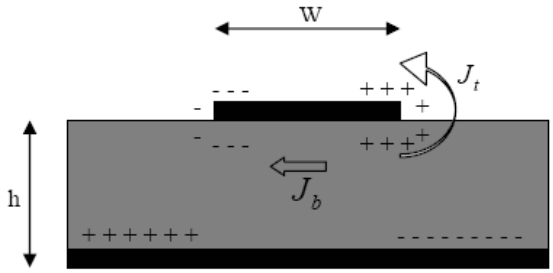

Fig. 2.11 Charge distribution and current density creation on the microstrip patch [1]

Consider Fig. 2.11 shown above. When the microstrip patch is provided power, a charge distribution is seen on the upper and lower surfaces of the patch and at the bottom of the ground plane. This charge distribution is controlled by two mechanisms – an attractive mechanism and a repulsive mechanism as discussed by Richards [17].

The attractive mechanism is between the opposite charges on the bottom side of the patch and the ground plane, which helps in keeping the charge concentration intact at the bottom of the patch. The repulsive mechanism is between the like charges on the bottom surface of the patch, which causes pushing of some charges from the bottom, to the top of the patch. As a result of this charge movement, currents flow at the top and bottom surfaces of the patch.

The cavity model assumes that the height to width ratio (ie. height of substrate and width of the patch) is very small and as a result of this the attractive mechanism dominates and causes most of the charge concentration and the current to be below the patch surface. Much less current would flow on the top surface of the patch and as the height to width ratio further decreases, the current on the top surface of the patch would be almost equal to zero, which would not allow the creation of any tangential magnetic field components to the patch edges. Hence, the four sidewalls could be modeled as perfectly magnetic conducting surfaces. This implies that the magnetic fields and the electric field distribution beneath the patch would not be disturbed. However, in practice, a finite width to height ratio would be there and this would not make the tangential magnetic fields to be completely zero, but they being very small, the side walls could be approximated to be perfectly magnetic conducting [1].

Since the walls of the cavity, as well as the material within the cavity are lossless, the cavity would not radiate and its input impedance would be purely reactive. Hence, in order to account for radiation and a loss mechanism, one must introduce a radiation resistance R_r and a loss resistance R_L. A lossy cavity would now represent an antenna and the loss is taken into account by the effective loss tangent δ_{eff} given by

$$\delta_{eff} = \frac{1}{Q_T} \tag{2.7}$$

where Q_T denotes the total antenna quality factor and has been expressed in [12] in the following form:

$$\frac{1}{Q_T} = \frac{1}{Q_d} + \frac{1}{Q_c} + \frac{1}{Q_r} \quad . \tag{2.8}$$

In Equation (2.8), the Q_d represents the quality factor of the dielectric and is given as

$$Q_d = \frac{\omega_r W_T}{P_d} = \frac{1}{\tan\delta} \tag{2.9}$$

where ω_r denotes the angular resonant frequency, W_T stands for the total energy stored in the patch at resonance, P_d represents the dielectric loss, and $\tan\delta$ is the loss tangent of the dielectric.

The Q_c represents the quality factor for radiation and is given as

$$Q_c = \frac{\omega_r W_T}{P_c} = \frac{h}{\Delta} \tag{2.10}$$

where P_c is the conductor loss, Δ is the skin depth of the conductor, and h is the height of the substrate.

The Q_r represents the quality factor for radiation and is given as

$$Q_r = \frac{\omega_r W_T}{P_r} \tag{2.11}$$

where P_r is the power radiated from the patch.

Substituting Equations (2.8), (2.9), (2.10) and (2.11) into Equation (2.7), we get

$$\delta_{eff} = \tan\delta + \frac{\Delta}{h} + \frac{P_r}{\omega_r W_T}. \tag{2.12}$$

Thus, Equation (2.12) describes the total effective loss tangent for the microstrip patch antenna.

2.4.3 Full Wave Solution – Method of Moments

One of the methods that provide the full wave analysis for the microstrip patch antenna is the Method of Moments. In this method, the surface currents are used to model the microstrip patch and the volume polarization currents are used to model the fields in the dielectric slab.

It has been shown by Newman and Tulyathan [18] how an integral equation is obtained for these unknown currents and using the Method of Moments, these electric field integral equations are converted into matrix equations which can then be solved by various algebraic techniques to provide the result. A brief overview of the Method of Moment described by Harrington [19] and [1] is given below.

The basic form of the equation to be solved by the Method of Moment is

$$F(g) = h \tag{2.13}$$

where F is a known linear operator, g is an unknown function, and h is the source or excitation function. The aim here is to find g, when F and h are known.

The unknown function g can be expanded as a linear combination of N terms to give:

$$g = \sum_{n=1}^{N} a_n g_n = a_1 g_1 + a_2 g_2 + ... + a_N g_N \tag{2.14}$$

where a_n is an unknown constant and g_n is a known function usually called a basis or expansion function.

Substituting Equation (2.14) into (2.13) and using the linearity property of operator F, we can write

$$\sum_{n=1}^{N} a_n F(g_n) = h \,. \tag{2.15}$$

The basis functions g_n must be selected in such a way that each $F(g_n)$ in the above equation can be calculated. The unknown constants a_n cannot be determined directly because there are N unknowns, but only one equation.

One method of finding these constants is the method of weighted residuals. In this method, a set of trial solutions is established with one or more variable parameters. The residuals are a measure of the difference between the trial solution and the true solution. The variable parameters are selected in a way that guarantees a best fit of the trial functions based on the minimization of the residuals. This is done by defining a set of N weighting (or testing) functions $\{w_m\} = w_1, w_2, \ldots\ldots\ldots w_N$ in the domain of the operator F. Taking the inner product of these functions, equation (2.15) becomes:

$$\sum_{n=1}^{N} a_n \langle w_m, F(g_n) \rangle = \langle w_{m,h} \rangle \tag{2.16}$$

where $m = 1, 2 \ldots\ldots N$.

Writing it in matrix form as shown in [1], we get:

$$[F_{mn}][a_n] = [h_m] \tag{2.17}$$

where

$$[F_{mn}] = \begin{bmatrix} \langle w_1, F(g_1) \rangle \langle w_1, F(g_2) \rangle \ldots\ldots\ldots\ldots \\ \langle w_2, F(g_1) \rangle \langle w_2, F(g_2) \rangle \ldots\ldots\ldots\ldots \\ \vdots \\ \vdots \end{bmatrix}, \quad [a_n] = \begin{bmatrix} a_1 \\ a_2 \\ a_3 \\ \vdots \\ a_N \end{bmatrix}, \text{ and } [h_m] = \begin{bmatrix} \langle w_1, h \rangle \\ \langle w_2, h \rangle \\ \langle w_3, h \rangle \\ \vdots \\ \langle w_N, h \rangle \end{bmatrix}.$$

The unknown constants a_n can now be found using algebraic techniques such as LU decomposition or Gaussian elimination. It must be remembered that the weighting functions must be selected appropriately so that elements of $\{w_n\}$ are not only linearly independent but they also minimize the computations required to evaluate the inner product. One such choice of the weighting functions may be to let the weighting and the basis function be the same, that is, $w_n = g_n$. This is known as the Galerkin's procedure as described by Kantorovich and Akilov [20].

From the antenna theory point of view, we can write the electric field integral equation (EFIE) as:

$$\underline{E} = f_e(\underline{J}) \tag{2.18}$$

where $\underline{E}$ is the known incident electric field, $\underline{J}$ is the unknown induced current, and f_e is the linear operator.

The first step in the moment method solution process would be to expand $\underline{J}$ as a finite sum of basis functions given as

$$\underline{J} = \sum_{i=1}^{M} J_i b_i \tag{2.19}$$

where b_i is the ith basis function and J_i is an unknown coefficient.

The second step involves the defining of a set of M linearly independent weighting functions, w_j. Taking the inner product on both sides and substituting Equation (2.19) into Equation (2.18) we get:

$$\left\langle w_j, \underline{E} \right\rangle = \sum_{i=1}^{M} \left\langle w_j, f_e(J_i, b_i) \right\rangle \tag{2.20}$$

where $j = 1,2,.....M$.

Writing it in matrix form, we have

$$\left[Z_{ij} \right] \left[\underline{J} \right] = \left[E_j \right] \tag{2.21}$$

where $Z_{ij} = \left\langle w_j, f_e(b_i) \right\rangle$, $E_j = \left\langle w_j, H \right\rangle$, and $\underline{J}$ is the current vector containing the unknown quantities.

The vector $\underline{E}$ contains the known incident field quantities and the terms of the $\underline{Z}$ matrix are functions of geometry. The unknown coefficients of the induced current are the terms of the $\underline{J}$ vector. Using any of the algebraic schemes mentioned earlier, these equations can be solved to give the current and then the other parameters such as the scattered electric and magnetic fields can be calculated directly from the induced currents. Thus, the moment method has been briefly explained for use in antenna problems.

2.5 Analysis of Antenna Arrays

In this thesis, a dual array patch antenna is examined similar to the one in [8]. Since the objective of the thesis is to improve bandwidth of a dual array patch antenna, a brief introduction to analysis of antenna arrays is given in subsequent sub-sections.

2.5.1 Simple Array Theory

Although a single element patch antenna may provide the desired antenna characteristics, combinations of many microstrip antennas into an array enable the

designer to fabricate microstrip antennas with high gain, beam shaping and beam steering capabilities. Control over such characteristics is only possible with the formation of antenna arrays.

Arrays of antennas usually consist of a repetition of radiating elements in a regular fashion. The elements may be identical or different and the structure may be configured as a linear, planar or volume array. Each element is also located at a specific distance from the other. The spacing between each element causes the fields from each element add or subtract in the far field to produce the desired radiation pattern. A practical reason supporting the feasibility of microstrip antenna arrays is the fact that conventional printed circuit etching processes are accurate, repeatable and relatively low in cost.

In the simple array theory, each radiator is first treated as a point isotropic source. The contributions from each point is derived in the far field and expressed as an array factor (AF). The array factor may be said to be the ‘standard’ pattern and depends only of the geometry of the array and the phase between each element. Each point is then replaced by the actual radiator and the far field radiation pattern is then determined by pattern multiplying the array factor with the pattern of the radiator. Mutual coupling is ignored in the process since the radiators are treated separately also their influence on each other are not considered. The simple array theory also does not account for the presence of other objects such as feed lines or obstructions.

2.5.2 Fixed Beam Linear Arrays

Consider a linear array of *M* uniformly-spaced elements located along the x-axis as shown in the coordinate system given in Fig. 2.12.

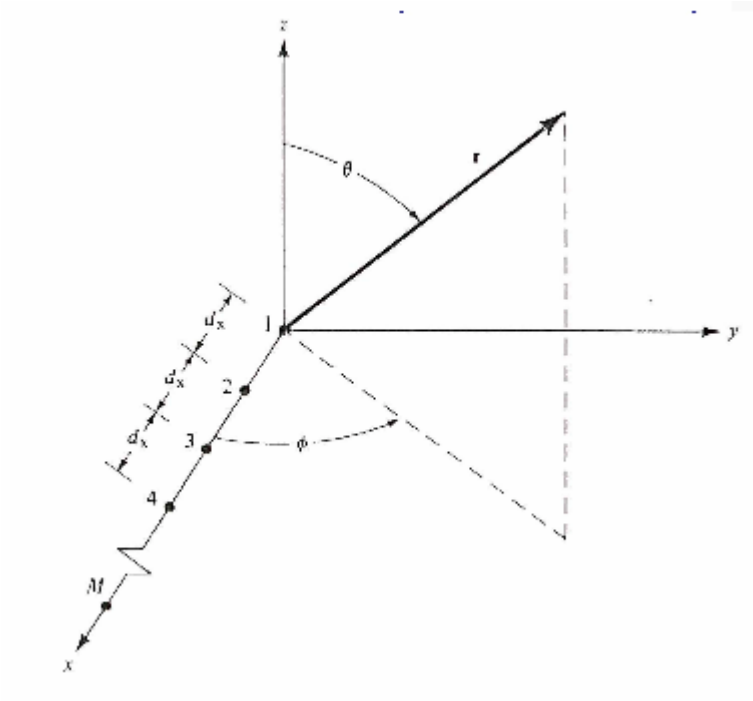

Fig. 2.12 Linear array geometry for patch antennas [1]

The array factor of such an array configuration may be written as

$$AF = \sum_{n=1}^{N} a_n e^{j(n-1)\psi} \tag{2.22}$$

$$\psi = kd\cos\gamma + \beta \tag{2.23}$$

where along axes x, y and z, we have

x-axis: $\cos\gamma = \hat{a}_x \cdot \hat{a}_r = \sin\theta\cos\phi$,

y-axis: $\cos\gamma = \hat{a}_y \cdot \hat{a}_r = \sin\theta\sin\phi$,

z-axis: $\cos\gamma = \hat{a}_z \cdot \hat{a}_r = \cos\theta$, respectively

and a_n is the excitation coefficient of each element. The array has a uniform spacing of d between each element as well as a progressive phase shift of β between the elements.

The normalized form of the array factor Equation (2.22) in the x-direction denoted by the subscript x may be written as

$$AF_x(\theta,\phi) = \frac{1}{M}\frac{\sin\left(\frac{M}{2}\psi_x\right)}{\sin\left(\frac{\psi_x}{2}\right)} \tag{2.24}$$

where $\psi_x = kd_x \sin\theta\cos\phi + \beta_x$.

Equation (2.24) is the form of the array factor used most often in pattern multiplication.

2.5.3 Planar Arrays

In the previous section, the array factor for a linear array was stated. Linear arrays (one dimensional) can scan the beam only in one plane. To scan the beam in any direction, two dimensional array geometries are needed, such as elements placed along a circle and planar, cubical, cylindrical, spherical, etc., surfaces.

The array factor for a planar array may be easily derived from the results in the linear array. Fig. 2.13 shows the geometry of a planar array.

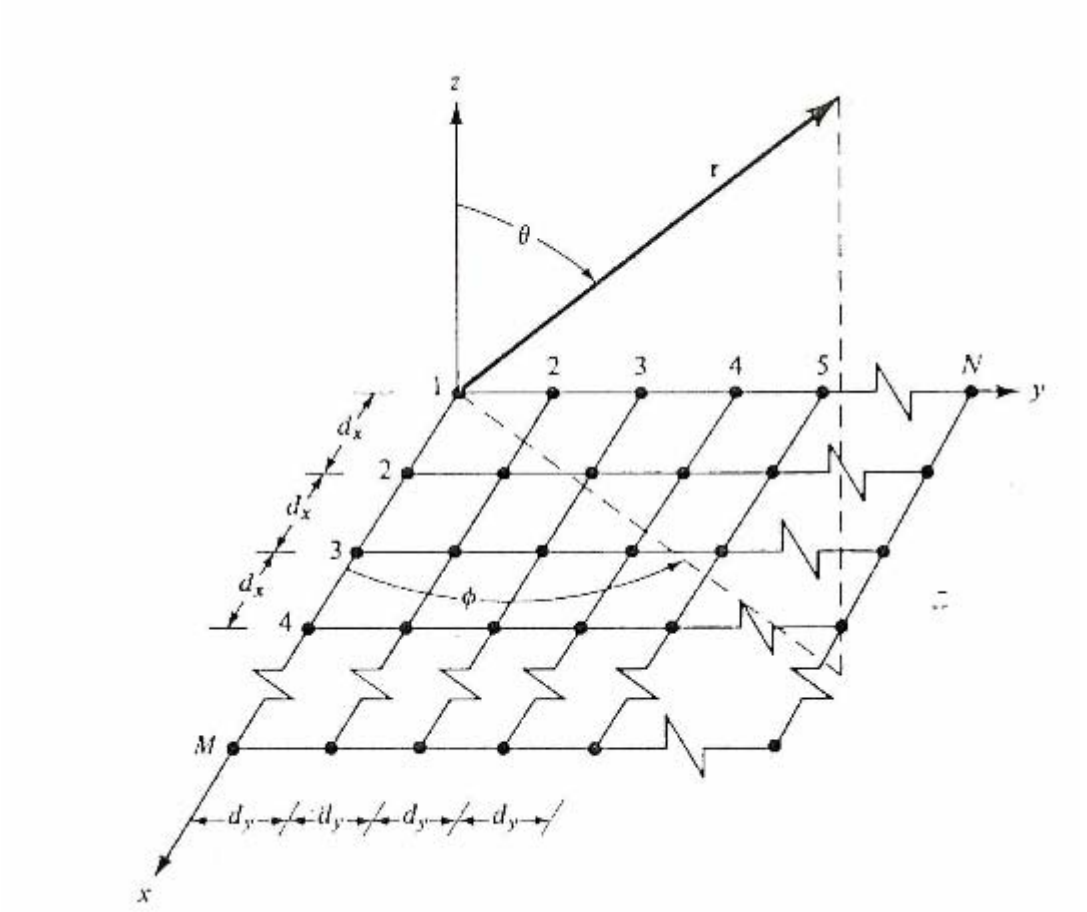

Fig. 2.13 Planar geometry for patch antennas [1]

By considering *N* linear arrays placed next to each other in the y-direction and spaced d_y apart, the normalized array factor can be obtained as

$$AF(\theta,\phi) = \left[\frac{1}{M}\frac{\sin\left(\frac{M}{2}\psi_x\right)}{\sin\left(\frac{\psi_x}{2}\right)}\right]\left[\frac{1}{N}\frac{\sin\left(\frac{N}{2}\psi_y\right)}{\sin\left(\frac{\psi_y}{2}\right)}\right] \qquad (2.25)$$

where $\psi_x = kd_x \sin\theta\cos\phi + \beta_x$ and $\psi_y = kd_y \sin\theta\cos\phi + \beta_y$.

2.6 Electromagnetic Bandgap (EBG) Structures

Electromagnetic bandgap (EBG) structures, also known as photonic bandgap (PBG) structures with origin in the area of optics [2] have attracted much attention among researchers in the microwave and antenna communities in the recent past. In general, EBG material is a periodic structure that forbids the propagation of all electromagnetic surface waves within a particular frequency band called the bandgap. Because of this, it permits an additional control of the behavior of electromagnetic waves other than conventional guiding and/or filtering structures. EBG has the potential to provide a simple and effective solution to the problems of surface and leaky waves.

EBG structures have been found to have a wide variety of applications in components of the microwave and millimeter wave devices, as well as in antennas [3]. In the recent years, various types of EBG structures have been studied for different applications [21]-[27].

In one of the first applications by using EBG materials to antennas, a planar antenna mounted only an EBG substrate was considered to increase the overall radiation efficiency of the device [21]. Increasing antenna directivity was studied using an EBG structure [22]. A mushroom like EBG structure was designed by Sievenpiper *et al.* [23]. This structure is characterized by having high surface impedance. A fork-like shape novel EBG structure was later studied [24] which is very compact in nature. The area of the fork-like structure was about 44% less than when compared to the conventional mushroom EBG structure. A compact spiral EBG structure was studied for microstrip antenna arrays [25], [26]. Spiral EBG structures, because of their

compact nature are very useful in wireless communications where size matters. These spiral EBG structures have also been examined to improve the performance of a triple band slot antenna [27] by etching them on the feedline.

The original EBG structure fabrication method needs painstaking work of drilling through the substrate in order to form periodic array of dielectric inclusions with a dielectric constant different from that of the host dielectric [2]. It costs a lot and time is wasted. Then comes the second method [28], which just etches the periodic lattice on the ground plane of microstrip line. This method is cheap and convenient.

In this thesis, the feedline of a dual patch microstrip antenna is etched with dummy EBG patterns. These patterns are termed as dummy EBG patterns because of their resemblance to the conventional EBG structures in certain properties and behavior. Even though these patterns are not etched on the ground plane like the conventional EBG structures, they appear to have similar properties like stopband features of an EBG structure. Also the number of elements that form the EBG patterns is not large; however it has been arranged in a periodic fashion similar to what one encounters in an EBG structure. The EBG structures helps in a reduction of the surface waves [11]. Also, the bandwidth enhancement can be due to the phenomena of slow wave characteristics. The EBG type structure exhibits slow wave characteristics in the passband near bandgap, i.e, a slow wave effect owing to the decrease of the propagation velocity $(LC)^{-\frac{1}{2}}$. It is based on increasing both distributed inductance L and capacitance C along feedline. At the same time, the average ratio of the inductance and capacitance should remain relatively constant for matching input and output lines.

2.7 Software Used

Computer-aided design (CAD) is fast becoming a norm in engineering today. This is because the use of such softwares helps to reduce development time by serving as a tool in the design process. Another reason is the increase in complexity in designs where accurate prediction of system performance can only be made with the help of CAD software packages.

In this project, Zeland's IE3D software is used [29]. IE3D is an integrated full-wave electromagnetic simulation and optimization package for the analysis and design of 3-dimensional microstrip antennas and high frequency printed circuits and digital boards (PCBs). As a method of moment (MOM) simulator, IE3D has many good features in modeling wide range structures such as microstrip circuits and antennas, strip-line circuits, CPW circuits and antennas, co-axial structure with uniform dielectric filling, inverted-F antennas, dipoles and other wire antennas, high speed transmission lines, high speed digital circuit interconnects, high speed digital circuit packaging. The primary formulation of the IE3D is an integral equation obtained through the use of Green's functions. IE3D can be used to model both the electric current on a metallic structure and a magnetic current representing the field distribution on a metallic aperture in a layered dielectric environment.

The software setting parameters are given below:

- Higher operating frequency: 18 GHz;
- Cells/wavelength ratio: 20

  (The higher the cells/wavelength ratio, the better is the accuracy of the simulated results obtained);

- Edge cell width to wavelength is put to be 0.1 in accordance with the design experiences.

2.8 Summary

In this chapter we discussed about patch antennas, its advantages and disadvantages, various feeding techniques and methods of analysis. After that, we introduced antenna arrays where we discussed about linear arrays and planar arrays. Next, theory on EBG structures was put forth and finally a brief introduction to Zeland's IE3D software used for simulation was given.

CHAPTER 3

DESIGN AND FABRICATION OF ANTENNAS

3.1 Introduction

In this chapter, design of different antenna structures is mentioned. The prototype or the reference antenna is a dual array patch antenna studied in [8]. Three different variations of this reference antenna are also designed each having different EBG patterns etched on the feedline connecting the two patches. All of these will be mentioned in subsequent sections.

3.2 Antenna Specifications

3.2.1 Choice of Substrate

Choosing a substrate is as crucial as the design itself. The substrate itself is part of the antenna and contributes significantly to its radiative properties. Many different factors are considered in choosing a substrate such as dielectric constant, thickness, stiffness as well as loss tangent. The dielectric constant should be as low as possible to encourage fringing and hence radiation. A thicker substrate should also be chosen since it increases the impedance bandwidth. However, using a thick substrate would incur a loss in accuracy since most microstrip antenna models use a thin substrate approximation in the analysis. Substrates which are lossy at higher frequencies should not be used for obvious reasons. The choice of a stiff or soft board basically depends on the application at hand.

3.2.2 Element Length

To chose the resonant length would also mean choosing the frequency of resonance since the resonant frequency of the patch is determined by the patch length. The length of the patch should be slightly less than half the dielectric wavelength since the actual patch is 'longer' due to the fringing fields. The length of the patch is given as

$$L = \frac{c}{2 f_r \sqrt{\varepsilon_{eff}}} - 2\Delta l \tag{3.1}$$

where f_r represents the resonant frequency and Δl represents the line extension at the ends given by Hammerstad [7] as

$$\Delta L = 0.412h \frac{\left(\varepsilon_{reff} + 0.3\right)\left(\frac{W}{h} + 0.264\right)}{\left(\varepsilon_{reff} - 0.258\right)\left(\frac{W}{h} + 0.8\right)}. \tag{3.2}$$

The effective dielectric constant ε_{eff} may be static or frequency dependent value.

3.2.3 Element Width

For an efficient radiator, Bahl [10] recommended using a practical element width given by

$$W = \frac{c}{2 f_0 \sqrt{\frac{\left(\varepsilon_r + 1\right)}{2}}}. \tag{3.3}$$

However, other widths may also be chosen especially if the widths are to be designed to radiate at a secondary frequency in dual-frequency operation. Square elements should be avoided in linearly polarized antennas to reduce the amount of cross polarization.

3.2.4 Input Impedance Matching

Impedance matching is critical in microstrip antennas since the bandwidth of the antenna depends upon it. Besides this, a poor match results in lower efficiency also. Line fed rectangular patches may be fed from the radiating or the non-radiating edge.

To find an impedance match along the non-radiating edge we may use the Transmission Line Model. The input impedance along the non-radiating edge is lowest at the centre since two equally high impedances at the two ends are transformed into a low value at the centre and connected in parallel. Matching along the edge is also symmetrical about the mid-point of the length. The input impedance at any location z along the edge may be determined by

$$Y_{in}(z) = 2G\left[\cos^2(\beta z) + \frac{G^2 + B^2}{Y_0^2}\sin^2(\beta z) - \frac{B}{Y_0}\sin(2\beta z)\right]^{-1}. \qquad (3.4)$$

The input impedance at the radiating edge is given by

$$Y_{in} = G + jB + Y_0\frac{G + j(B + Y_0\tan\beta L)}{Y_0 + j(G + jB)\tan\beta L}. \qquad (3.5)$$

3.2.5 Considerations for Antenna Arrays

The spacing between the antenna elements plays a major role in the design. Too large a spacing results in the presence of grating lobes which is undesirable in most instances. On the other hand, too close a spacing leads to broader beamwidth which may be unacceptable. Smaller spacings also reduce the amount of space for the feed network. Hence the space between the elements should be adjusted properly. To obtain maximum additive radiating fields the separation between the elements should be about $\lambda/2$.

3.2.6 Antenna Specifications

Based on the above design considerations:

Thickness of the substrate (*h*): 0.381 mm (0.02λ).

Patch size : 8 mm (0.4λ) by 6.3 mm (0.315λ)

Substrate dielectric (ε_r) : 2.33

Antenna resonating frequency: 14.8 GHz

Antenna gain : 9.5 dBi

Antenna bandwidth : 0.26 GHz

Antenna Efficiency : 80 %

Input Impedance : 50 Ω

3.3 Reference Antenna

Reference antenna or the prototype antenna is the basic antenna that will be used for comparison of different results with the other proposed EBG patterned antennas. The reference antenna is similar to the one examined in [8]. It is a dual array patch antenna with no EBG pattern etched on the feedline connecting the two patches.

Using Equations (3.1), (3.2) and (3.3), the length and width of the reference or the prototype antenna is found to be 8 mm (0.4λ) and 6.3 mm (0.315λ), respectively. A quarter wave transformer ($\lambda/4$) is used for matching purposes whose width is 1.9 mm (0.095λ) and length is 3.6 mm (0.18λ). Fig. 3.1 shows the structure of the reference antenna, where Fig. 3.1(a) shows the antenna layout while Fig. 3.1(b) shows the fabricated antenna. The dimensions of the antenna are shown in the figure itself.

Different variations of this reference antenna are also found by shifting the position of the feedline connecting the two patches to various locations by IE3D simulation software. This is highlighted in Fig. 3.1 by the parameter "s" that we change. These variations will be used in determining the significance of the position of feedline on bandwidth which will be mentioned in Chapter 4. Fig. 3.1 shows one of these variations that has been found to have the best result in terms of maximum improvement in bandwidth when compared to EBG patterned antenna.

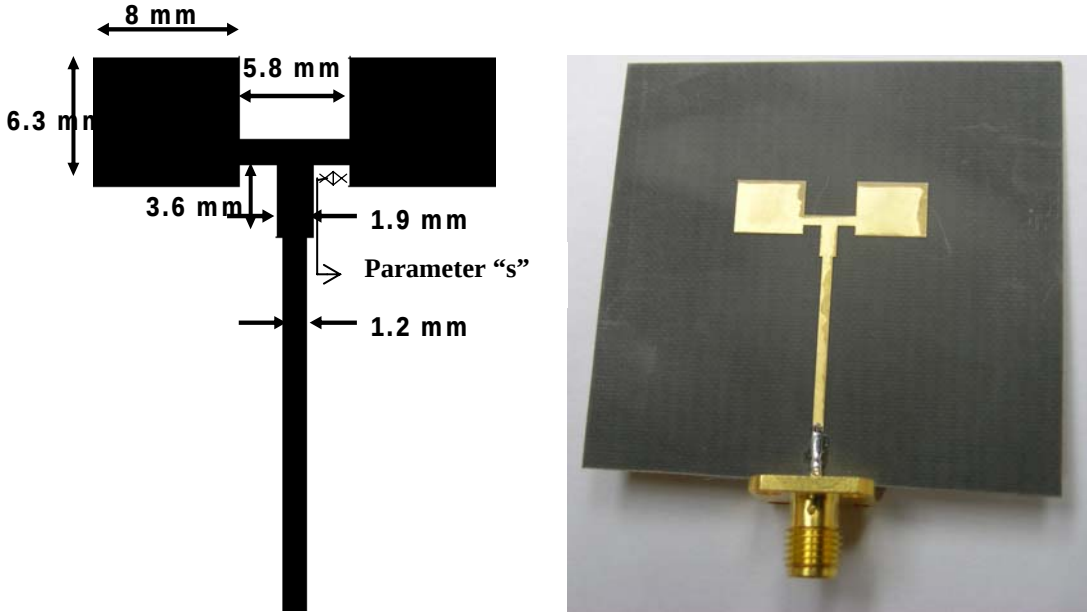

(a) Antenna layout (b) Fabricated antenna

Fig. 3.1 Reference antenna

3.4 Antenna Variations

Three different variations of the reference antenna are designed by etching different EBG patterns on the feedline connecting the twin patches. These variations are termed as antenna variant-1, antenna variant-2 and antenna variant-3 each having EBG pattern-1, EBG pattern-2 and EBG pattern-3, respectively. The patch dimensions,

substrate thickness and dielectric constant of each of these antenna variants are similar to the reference antenna.

An array of 2x4 similar patterns is etched on the feedline connecting the two patches of the reference antenna. The array is built on a 0.381 mm (0.02λ) thick substrate with the relative permittivity of 2.33. The period of all the proposed patterns is 0.8 mm (0.04λ), which is operating at a frequency of about 14.8 GHz. As such, the period of the pattern is about 4% of the wavelength at the stopband frequency, which satisfies the conventional definition for an EBG structure. Because these array patterns behave similar to EBG structures, they have been termed as dummy EBG patterns.

3.4.1 Antenna Variant-1

The proposed antenna variant-1 is shown in Fig. 3.2, where Fig. 3.2(a) shows the antenna layout and Fig. 3.2(b) shows the fabricated antenna.

(a) Antenna layout (b) Fabricated antenna

Fig. 3.2 Antenna variant-1

The magnified view of the feedline for antenna variant-1 in Fig. 3.2 is shown in Fig. 3.3, where Fig. 3.3(a) shows the feedline layout for antenna variant-1 and Fig. 3.3(b) shows the magnified view of the feedline in the fabricated antenna. Note that only a small part of the antenna patches are shown in Fig. 3.3.

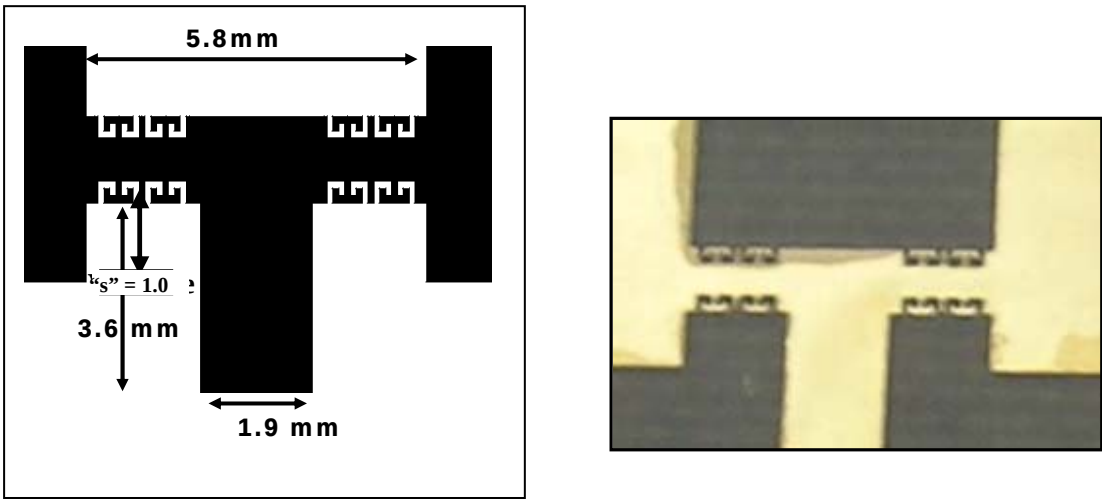

(a) Feedline layout (b) Fabricated antenna

Fig. 3.3 Magnified view of the feedline of antenna variant-1

The proposed EBG pattern that has been etched in an array fashion on the feedline of the antenna is shown in Fig. 3.4. This pattern resembles two English alphabets “E” joined together in opposite fashion and hence has been termed as – “Opposite Double-E Dummy EBG Pattern” or EBG pattern-1. The dimensions of EBG pattern-1 have been tabulated in Table 3.1.

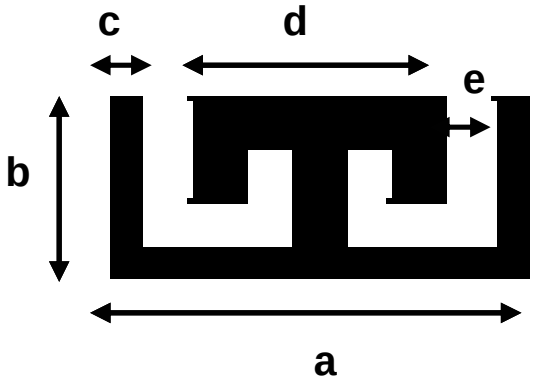

Fig. 3.4 Single EBG pattern-1 etched on feedline of antenna variant-1

3.4.2 Antenna Variant–2

The proposed antenna variant-2 is shown in Fig. 3.5, where Fig. 3.5(a) shows the antenna layout and Fig. 3.5(b) shows the fabricated antenna.

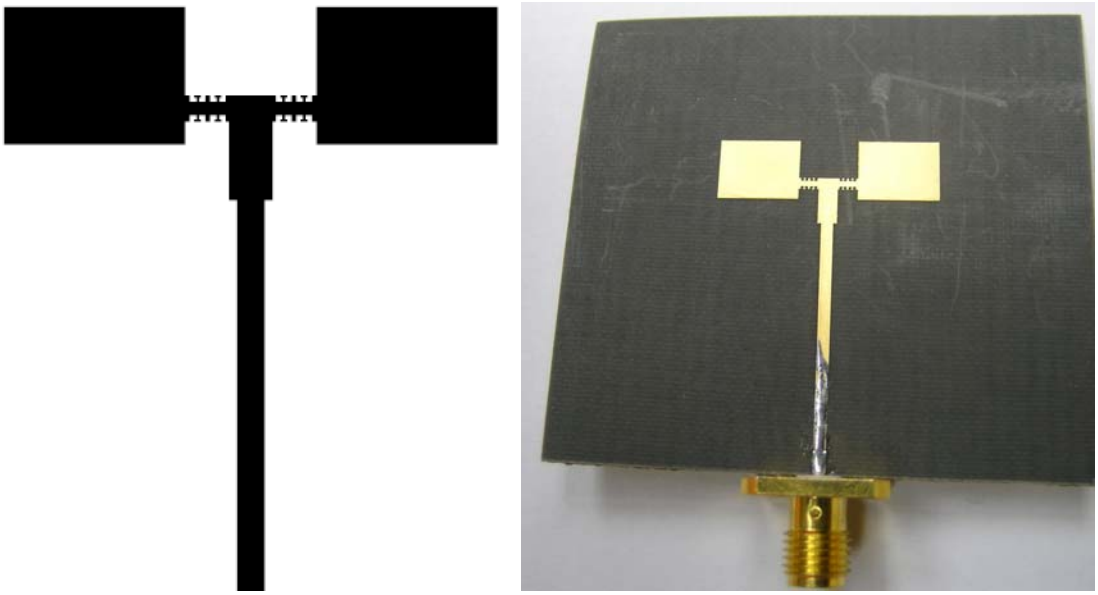

(a) Antenna layout (b) Fabricated antenna

Fig. 3.5 Antenna variant-2

The magnified view of the feedline for antenna variant-2 in Fig 3.5 is shown in Fig. 3.6, where Fig. 3.6(a) shows the feedline layout for antenna variant-2 and Fig. 3.6(b)

shows the magnified view of the feedline in the fabricated antenna. Note that only part of the antenna patches are shown in Fig. 3.6.

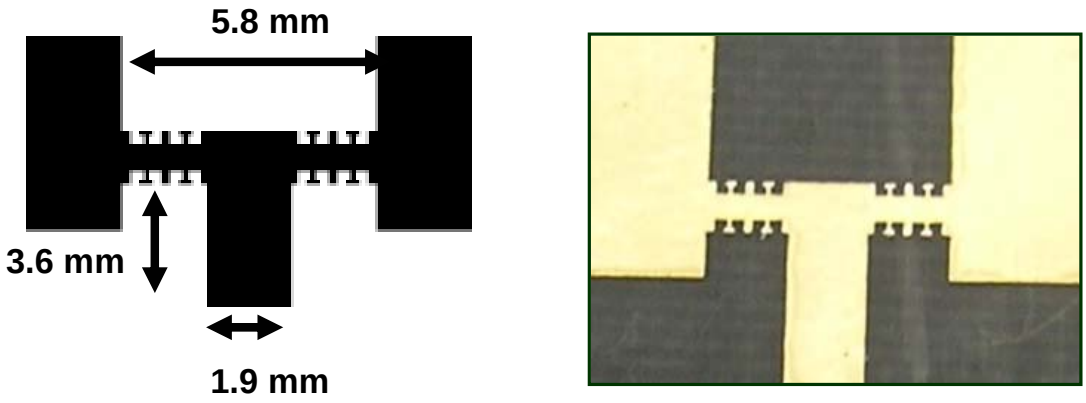

(a) Feedline layout (b) Fabricated antenna

Fig. 3.6 Magnified view of the feedline of antenna variant-2

The proposed pattern that has been etched in an array fashion on the feedline of the antenna is shown in Fig. 3.7. This pattern is similar to pattern-1 with minor changes. The pattern resembles a Top hat structure and has been termed as “Top Hat dummy EBG pattern” or EBG pattern-2. The dimensions of EBG pattern-2 have also been been tabulated in Table 3.1.

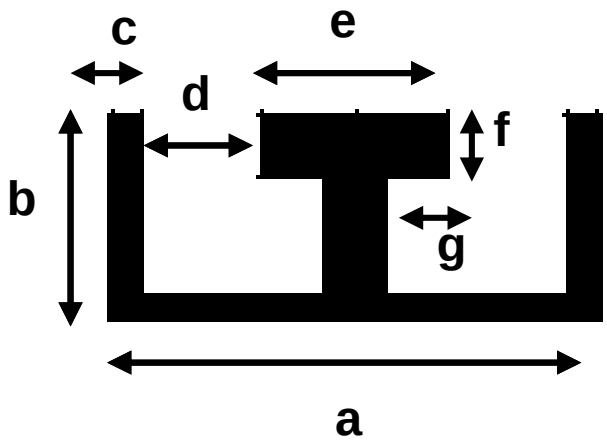

Fig. 3.7 Single EBG pattern-2 etched on feedline of antenna variant-2

3.4.3 Antenna Variant–3

The proposed antenna variant-3 is shown in Fig. 3.8, where Fig. 3.8(a) shows the antenna layout and Fig. 3.8(b) shows the fabricated antenna.

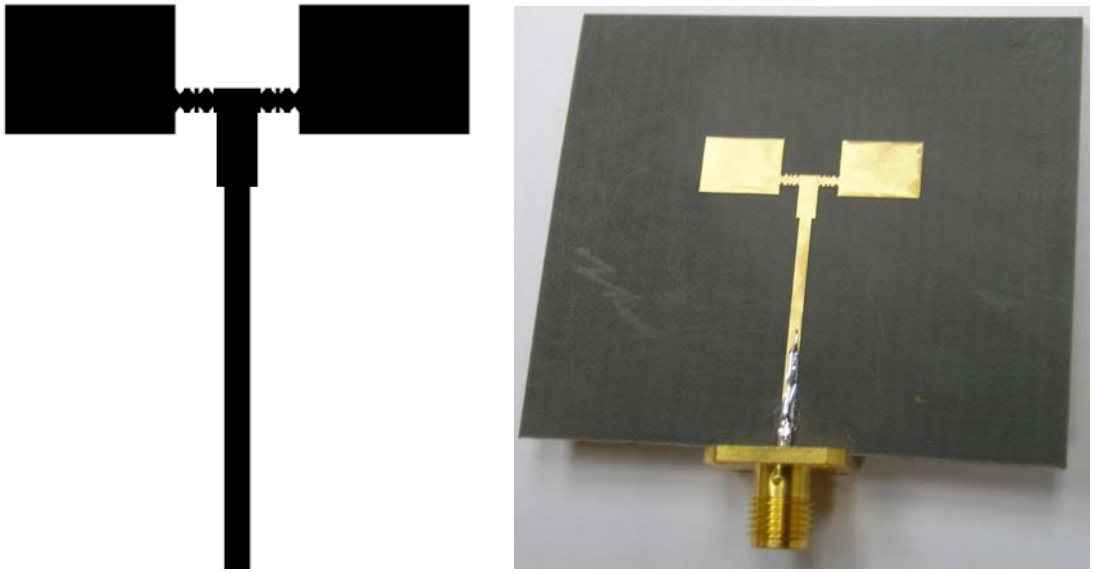

(a) Antenna layout (b) Fabricated antenna

Fig. 3.8 Antenna variant-3

The magnified view of the feedline for antenna variant-3 in Fig. 3.8 is shown in Fig. 3.9, where Fig. 3.9(a) shows the feedline layout for antenna variant-3 and Fig. 3.9(b) shows the magnified view of the feedline in the fabricated antenna. Note that only part of the antenna patches are shown in Fig. 3.9.

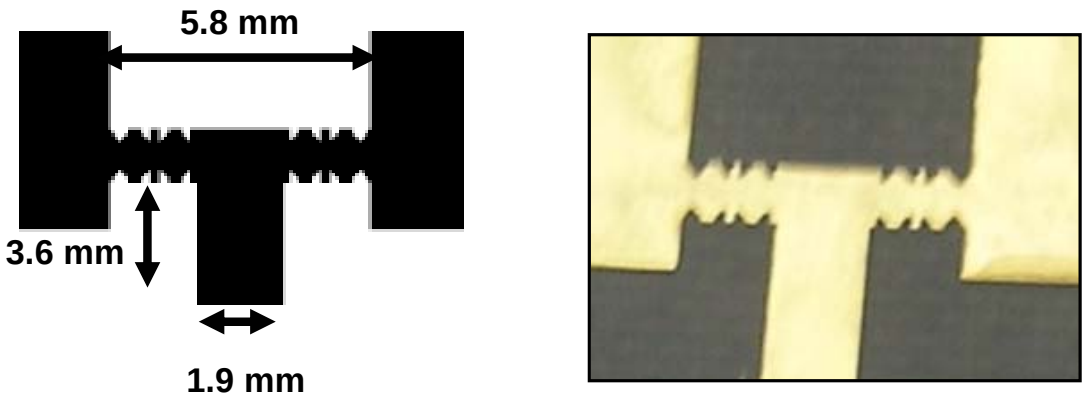

(a) Feedline layout (b) Fabricated antenna

Fig. 3.9 Magnified view of feedline of antenna variant-3

The proposed pattern that has been etched in an array fashion on the feedline of the antenna is shown in Fig. 3.10. The pattern resembles a hut structure and hence has been termed as “Hut-shaped EBG pattern” or EBG pattern-3. The dimensions of EBG pattern-3 have been tabulated in Table 3.1.

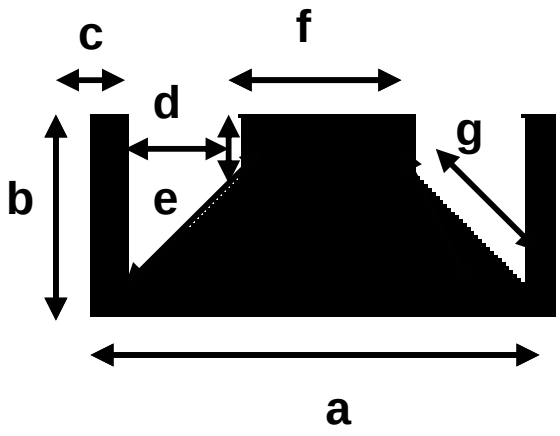

Fig. 3.10 Single EBG pattern-3 etched on feedline of antenna variant-3

Table 3.1 tabulates the physical parameters for different EBG patterns. The dimensions used are in millimeter (mm).

TABLE 3.1: Physical parameters of EBG patterns etched on feedline for different antenna variants

Antenna	Normalized Frequency & length in (mm) at 14.8 GHz						
	a	b	c	d	e	f	g
EBG Pattern-1	0.04 λ (0.8)	0.0175 λ (0.35)	0.0025 λ (0.05)	0.025 λ (0.5)	0.005 λ (0.1)	-	-
EBG Pattern-2	0.04 λ (0.8)	0.0175 λ (0.35)	0.0025 λ (0.05)	0.01 λ (0.2)	0.015 λ (0.3)	0.005 λ (0.1)	0.005 λ (0.1)
EBG Pattern-3	0.04 λ (0.8)	0.0175 λ (0.35)	0.0025 λ (0.05)	0.01 λ (0.2)	0.005 λ (0.1)	0.015 λ (0.3)	0.014 λ (0.28)

Note that antenna variant–1, antenna variant–2 and antenna variant–3 will be used interchangeably with antenna structure-1, antenna structure–2 and antenna structure-3, respectively in the thesis.

3.5 Summary

In this chapter, design procedure of different antennas such as reference antenna and its three variants, namely, antenna variant-1, antenna variant-2 and antenna variant-3 are provided. The reference antenna is a dual array patch antenna operating at a high frequency. The three variants have different EBG patterns etched on the feedline.

CHAPTER 4

RESULTS & DISCUSSIONS

4.1 Introduction

In this chapter, we will discuss important results obtained for reference antenna and its three variants. Firstly, in Section 4.2, we investigate the significance of the position of feedline connecting the twin patches of the dual array patch antenna with respect to the bottom of the twin patches. We find the optimum position of the feedline for our antenna design that is useful to have the maximum improvement in bandwidth.

Next, in Section 4.3, we discuss S_{11} parameters, bandwidth, current distribution, radiation patterns and other important antenna parameters such as antenna efficiency, radiation efficiency and antenna gain for all the antenna structures obtained from simulation and measurement. It will be shown that a significant improvement in bandwidth can be obtained by etching feedline with EBG patterns.

4.2 Significance of Feedline Position

In this section we investigate the significance of the position of the feedline connecting the twin patches. Reference antenna and antenna variant-1 are used for the simulation purpose to come up with the results.

The feedline positions for both the reference antenna and antenna variant-1 are shifted to various positions with respect to the bottom of the patch. Care has been taken to match the circuit properly when shifting the feedline position. Zeland's IE3D version 12's inbuilt features are used for this purpose. By shifting the feedline, we obtain a

subset of antenna structures each for reference antenna and antenna variant-1, all having different feedline positions/distances measured from the bottom of the twin patches.

We obtain different results for S_{11} parameters and bandwidth values for each subset antenna structure of reference antenna and each subset antenna structure of antenna variant-1. Here, we compare 5 best cases found out from simulation results.

The position of the feedline measured from bottom of the patch is changed and fixed at 1.0 mm, 1.05 mm, 1.1 mm, 4.05 mm and 4.1 mm for the reference antenna and antenna variant-1. Hence, we obtain 5 subsets of reference antenna having different feed positions and 5 subsets of antenna variant-1 having different feed positions as mentioned previously. The S_{11} parameter graphs for subset reference antenna and subset antenna variant-1 for same feed position are shown and compared in Fig. 4.1, where Figs. 4.1(a), 4.1(b), 4.1(c), 4.1(d) and 4.1(e) correspond to feed positions 1.0 mm, 1.05 mm, 1.1 mm, 4.05 mm and 4.1 mm, respectively.

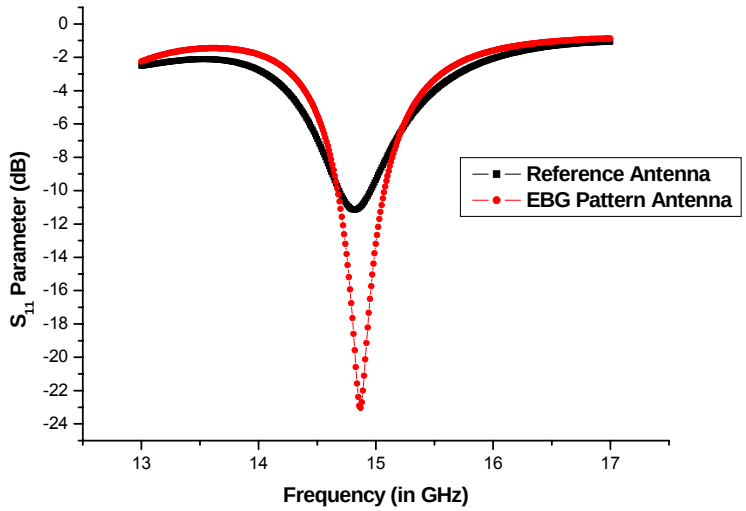

(a) Feedline position at 1.0 mm measured from bottom of patch

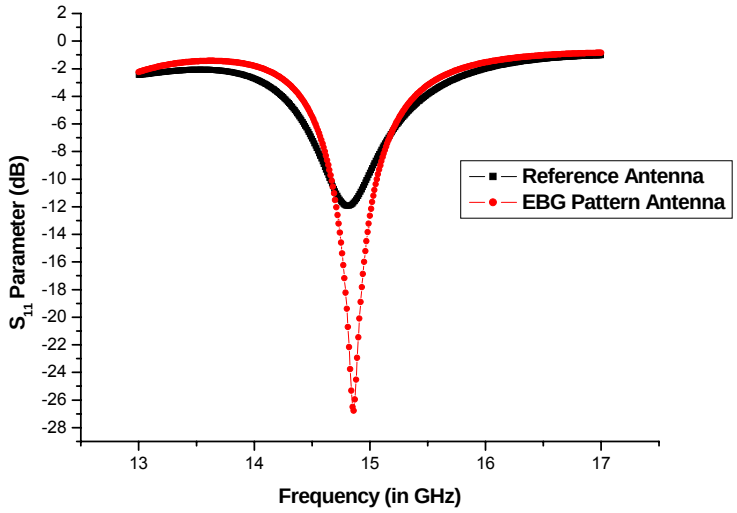

(b) Feedline position at 1.05 mm measured from bottom of patch

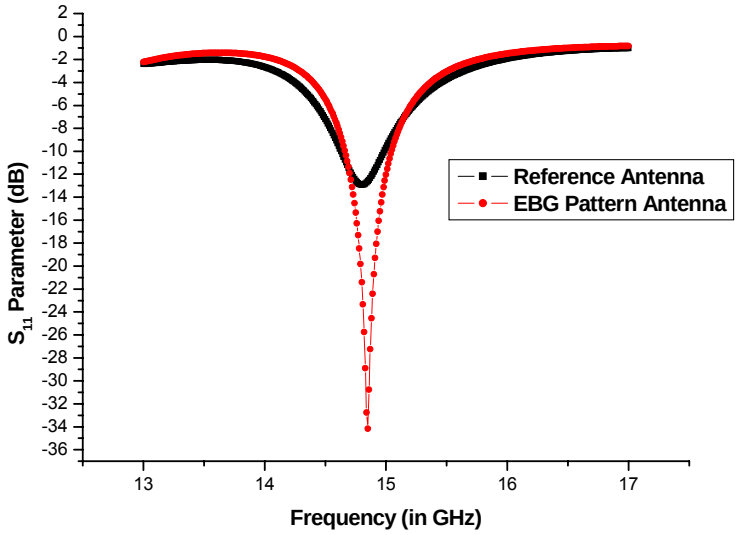

(c) Feedline position at 1.1 mm measured from bottom of patch

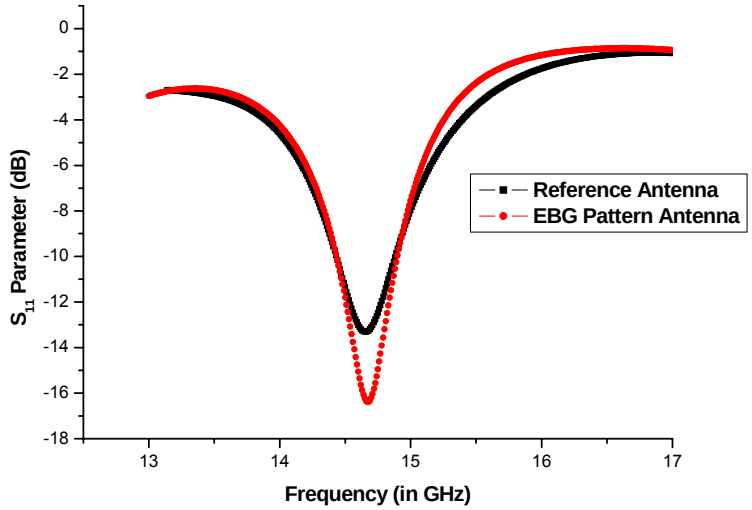

(d) Feedline position at 4.05 mm measured from bottom of patch

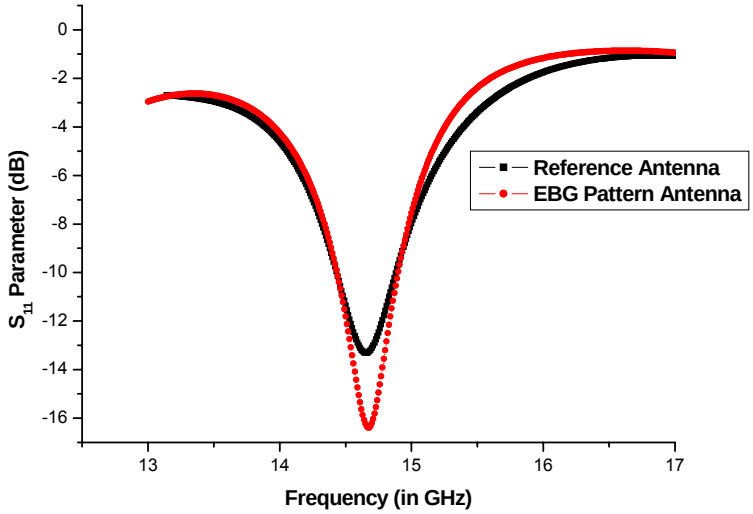

(e) Feedline position at 4.1 mm measured from bottom of patch

Fig. 4.1 S_{11} parameter value Vs frequency (in GHz) comparison of reference antenna with antenna variant-1 for 5 different feed positions

Table 4.1 shows the S_{11} parameter comparison for reference antenna and antenna variant-1 for different feed positions while Table 4.2 shows the bandwidth comparison for different feed positions.

Table 4.1: S_{11} parameter values obtained at the central frequency (14.8 GHz) through simulation for reference antenna and antenna variant-1

Feedline Distance (Measured from bottom of twin patch)	Reference Antenna	Antenna variant-1 (With EBG pattern-1)
1.0 mm	-11.15 dB	-23.03 dB
1.05 mm	-11.94 dB	-26.76 dB
1.1 mm	-12.92 dB	-34.17 dB
4.05 mm	-13.42 dB	-15.18 dB
4.1 mm	-12.44 dB	-16.39 dB

The S_{11} parameter is a measure of the reflected signal when we inject a signal at port 1 of the antenna. For good matching, S_{11} should be better than -10 dB in the passband range. From Table 4.1 we observe that S_{11} parameter value is increased considerably for antenna variant-1, i.e. antenna with EBG pattern-1, when compared to the reference antenna for the same feedline position when the feedline position is closer to the lower edge of the twin patch (distances 1.0 mm, 1.05 mm and 1.1 mm measured from bottom of twin patch).

Table 4.2: Bandwidth (BW) comparison for different subsets of reference antenna and antenna variant-1 for 5 different cases (different feedline positions) for central frequency of 14.8 GHz

No	Feedline distance (from the bottom of the patch)	Reference Antenna (BW)	Antenna Variant-1 (with EBG pattern-1) (BW)	Percentage change in BW
1	1.0 mm	0.2682	0.3987	48.7 %
2	1.05 mm	0.3199	0.3932	22.9 %
3	1.1 mm	0.3551	0.3849	8.4 %
4	4.05 mm	0.4399	0.4643	5.5 %
5	4.1 mm	0.4289	0.4575	6.7 %

From Table 4.2, we observe that for the reference antenna, when the position of the feedline is closer to the upper edge of the twin patch, we obtain a greater bandwidth in comparision with the bandwidth obtained when the feedline is closer to the lower edge. Note that during the process of shifting the feedline from the lower edge to the upper edge of the twin patch, the geometry of the feedline is changed because of the change in the matching circuit. This was done using inbuilt features in IE3D software. Hence, these two antenna systems are different in geometry.

Also, from Table 4.2, we find that for the antenna variant-1, we obtain a different trend in bandwidth as compared to the reference antenna. For antenna variant-1, even though the bandwidth obtained when the feedline is closer to the upper edge is greater than when the feedline is closer to the lower edge, the difference is not much. The sensitivity of bandwidth to the change in feedline position is reduced. However, note that the geometries of these antenna variant's-1 are changed when the feedline is shifted to different locations due to the change in matching circuit as discussed previously.

The major concern of the thesis is to improve the bandwidth of the reference antenna by using dummy EBG patterns without changing the antenna geometry. Hence, we consider comparing reference antenna and antenna variant-1 for the same feedline position as the matching circuit and geometry is same for the 2 antenna structures. We observe that when the position of the feedline is closer to the lower edge of the patch, we obtain a maximum improvement in bandwidth for the antenna variant-1 when compared with the reference antenna for the same feedline position. This has been verified in the last column of Table 4.2.

The best position obtained is 1.0 mm (0.05λ) measured from the bottom of the twin patch. Reference antenna and antenna variant-1 when the feedline position is 1.0 mm (0.05λ) measured from the bottom of the twin patch are fabricated. This has been shown in Fig. 3.1 and Fig. 3.2, respectively in Chapter 3.

4.3 Measurement Results and Discussions

In this section, we obtain a comparison of results for the reference antenna and its three variants, namely, antenna variant-1, antenna variant-2 and antenna variant-3, for feedline position 1.0 mm measured from the bottom of the twin patch. These will be shown in subsequent subsections.

4.3.1 Antenna Variant-1 Vs Reference Antenna

4.3.1.1 S_{11} Parameters

The S_{11} parameter value Vs frequency in GHz graph for the reference antenna and antenna variant-1 is shown in Fig. 4.2.

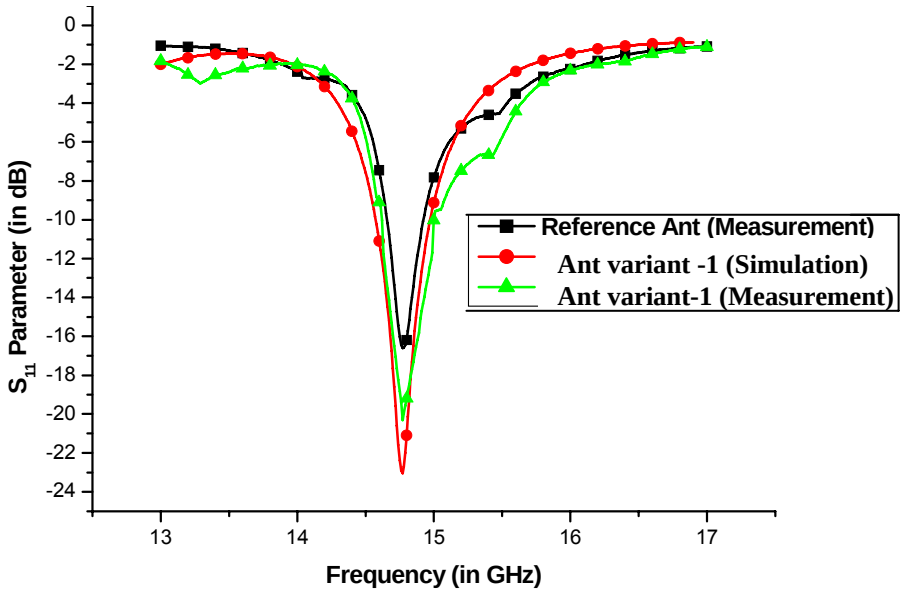

Fig. 4.2 S_{11} parameter Vs frequency Graph obtained from measurement for reference antenna and antenna variant-1 having EBG pattern-1

The simulated and measured S_{11} parameter values for reference antenna and antenna variant-1 are tabulated in Table 4.3.

Table 4.3: S_{11} parameter results for reference antenna and antenna variant-1 obtained from simulation and measurement at central frequency of 14.8 GHz

	Simulation Result	Measurement Result
Reference Antenna	-11.15 dB	-16.5 dB
Antenna variant-1	-23.03 dB	-20.8 dB

From Table 4.3, we observe that the simulated and measured results are in agreement with each other. The S_{11} parameter values obtained are greater than -10 dB in the passband range which is a desirable result.

4.3.1.2 Bandwidth

The bandwidths of the reference antenna and antenna variant-1 are obtained from simulation and measurement. The bandwidths of the antennas are tabulated in Table 4.4. Both simulation and measurement results are in agreement with each other.

Table 4.4: Bandwidth results for reference antenna and antenna variant-1 obtained from simulation and measurement at central frequency of 14.8 GHz

	Simulation Result	Measurement Result
Reference Antenna	0.2682 GHz	0.256 GHz
Antenna Variant-1	0.3987 GHz	0.381 GHz

From Table 4.4, we observe that by etching EBG pattern-1 in antenna structure-1 we can improve the bandwidth by upto 48% when compared with the reference antenna having no EBG pattern. The EBG pattern is shown in Fig. 3.4 in Chapter 3. Thus, a considerable improvement in bandwidth can be obtained for the same feedline position.

4.3.1.3 Current Distribution

Current distribution graphs for the reference antenna and antenna variant-1 is obtained and shown in Fig. 4.3, where Fig. 4.3(a) shows the current distribution for reference antenna while Fig. 4.3(b) shows the current distribution for antenna variant-1.

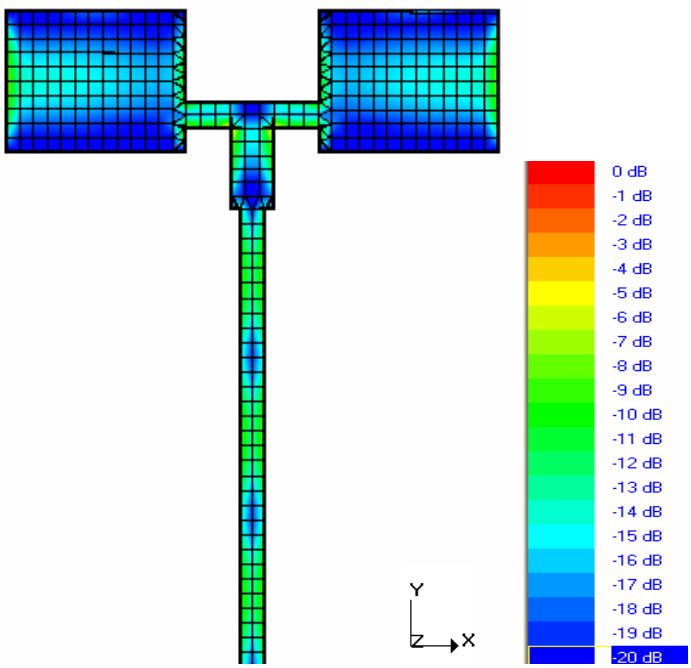

(a) Reference antenna

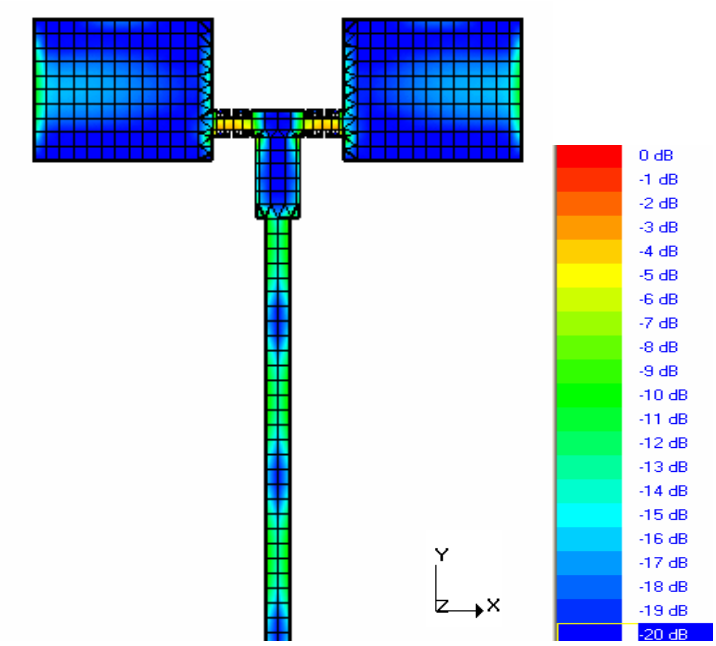

(b) Antenna variant-1

Fig. 4.3 Current distribution for reference antenna and antenna variant-1

From Fig. 4.3, we see that at and near the EBG patterns the magnitude of current distribution is minimized. This is because when we etch the antenna with the EBG structure, we are changing the antenna impedance. An antenna is a structure carrying an electrical current and the electrical properties of the antenna depends upon the distribution of that current in magnitude and phase. When the current distribution of the antenna is changed, it also changes its characteristics as shown in Table 4.5.

4.3.1.4 Radiation Patterns

Radiation patterns are obtained by measurement for reference antenna and antenna variant-1. Both *E*-plane and *H*-plane patterns are obtained. The radiation pattern for reference antenna is shown in Fig. 4.4 while that for antenna variant-1 is shown in Fig. 4.5. Cross polarization measurement results are also shown in the figure.

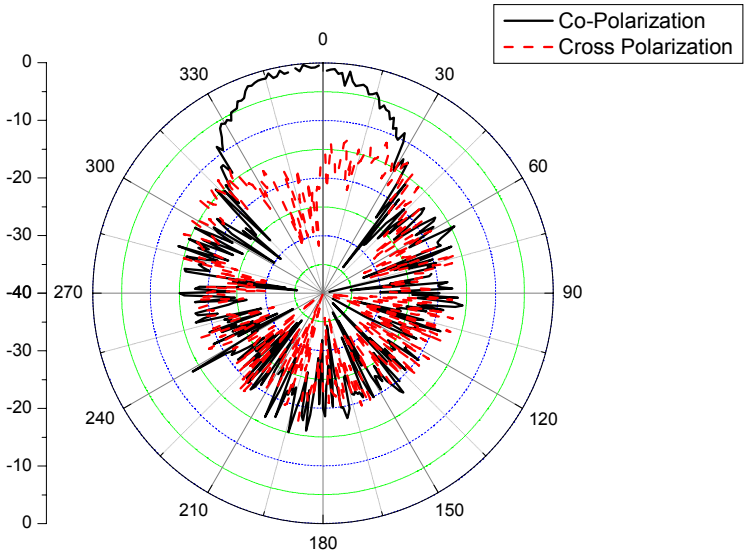

(a) *E* Plane

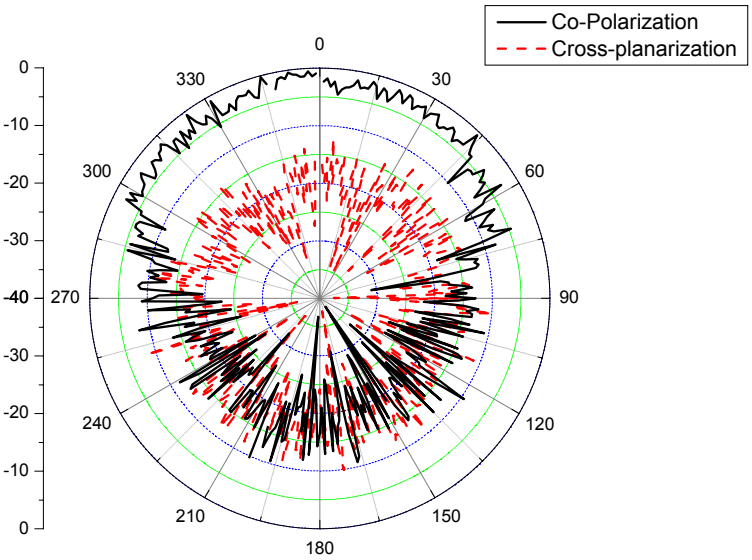

(b) *H* Plane

Fig. 4.4 Radiation pattern *E* plane and *H* plane for reference antenna measured at 14.8 GHz

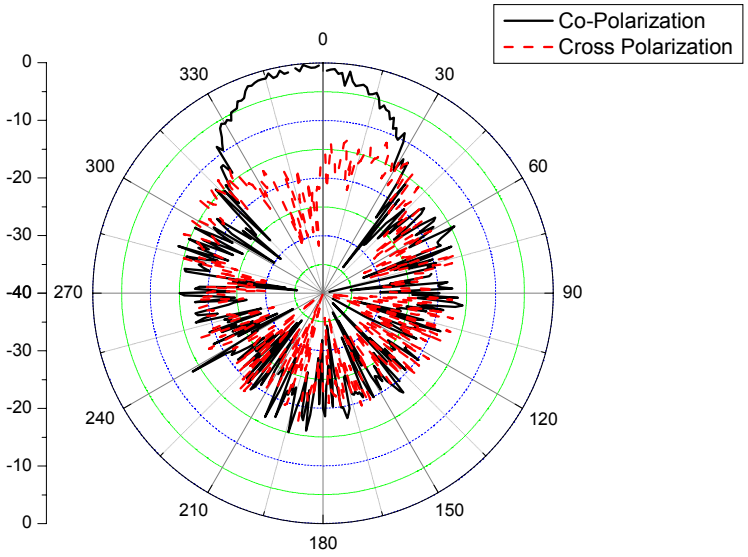

(a) *E* Plane

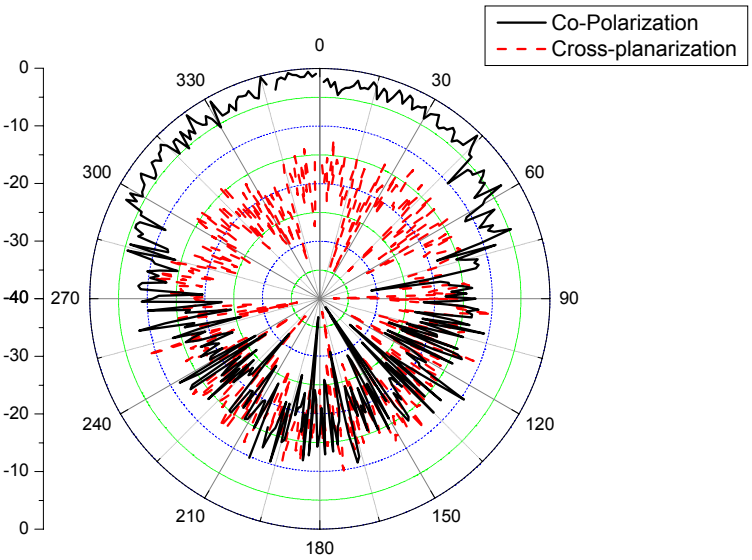

(b) *H* Plane

Fig. 4.5 Radiation pattern *E* plane and *H* plane for antenna variant-1 measured at 14.8 GHz

From Figs. 4.4 and 4.5, we observe that the respective *E*-plane and *H*-plane of the reference antenna and antenna variant-1 do not significantly change. This is expected

as radiation is due to the twin patches and these patches do not change for the two antenna structures.

Due to the limitation of the measurement chamber, significant noise is observed in the measurement results. The attenuation of signal in the chamber, where measurements were obtained, is very large for operating frequency above 10 GHz. Since, the radiation patterns are obtained at a frequency of 14.8 GHz, we experience a high attenuation. Hence, it is difficult to get results with minimum noise and smooth curve. The cross polarization plot is also shown in Figs. 4.5 and 4.6. It is comparatively lower than the co-polarization or the main polarization.

4.3.1.5 Other Antenna Parameters

Some other important antenna parameters namely radiation efficiency, antenna efficiency and linear gain are obtained and compared for reference antenna and antenna variant-1 and have been tabulated in Table 4.5.

Table 4.5: Other important antenna parameters for reference antenna and antenna variant-1 at central frequency of 14.8 GHz

Antenna Performance	Reference Antenna	Antenna variant-1
Radiation Efficiency	88.58%	88.95%
Antenna Efficiency	81.71%	87.11%
Linear Gain	9.71 dBi	9.94 dBi

From Table 4.5, we see that radiation efficiency of antenna structures, reference antenna and antenna variant-1, are almost similar. However, there is an improvement

in antenna efficiency and gain for the antenna with dummy EBG pattern (antenna variant-1) when compared to the reference antenna.

Antenna efficiency is defined as the product of reflection efficiency, conduction efficiency and dielectric efficiency. Since, conduction and dielectric efficiency are difficult to separate, these are generally lumped together to form antenna radiation efficiency. Hence, antenna efficiency is a product of reflection efficiency and radiation efficiency. From Table 4.5 we observe that radiation efficiency remains almost the same whereas antenna efficiency increases. Thus, we can say that reflection efficiency has been increased which leads to a greater antenna efficiency.

Gain (G) is related to directivity (D) of antenna. Directivity is how much an antenna concentrates energy in one direction in preference to radiation in other directions. Hence, if antenna is 100% efficient, then directivity would be equal to gain and the antenna would be an isotropic radiator. Since all antennas will radiate more in some direction than in others, therefore the gain is the amount of power that can be achieved in one direction at the expense of the power lost in the others. From Table 4, we see that gain of the feedline etched antenna is improved which is desirable.

4.3.2 Antenna Variant-2 Vs Reference Antenna

Here, we obtain and compare measurement results with simulation results for antenna variant-2 and reference antenna. S_{11} Parameter, bandwidth, current distribution, radiation patterns and some other important antenna parameters will be discussed. The feedline positions for reference antenna and antenna variant-2 are fixed both at a distance of 1.0 mm measured from the bottom of the twin patch. The fabricated

antenna variant-2 used for obtaining measurement results has been shown in Fig. 3.5 in Chapter 3.

4.3.2.1 S_{11} Parameters

The S_{11} parameter value Vs frequency in GHz graph for the reference antenna and antenna variant-2 is shown in Fig. 4.6. Both simulation and measurement results are shown in Fig. 4.6.

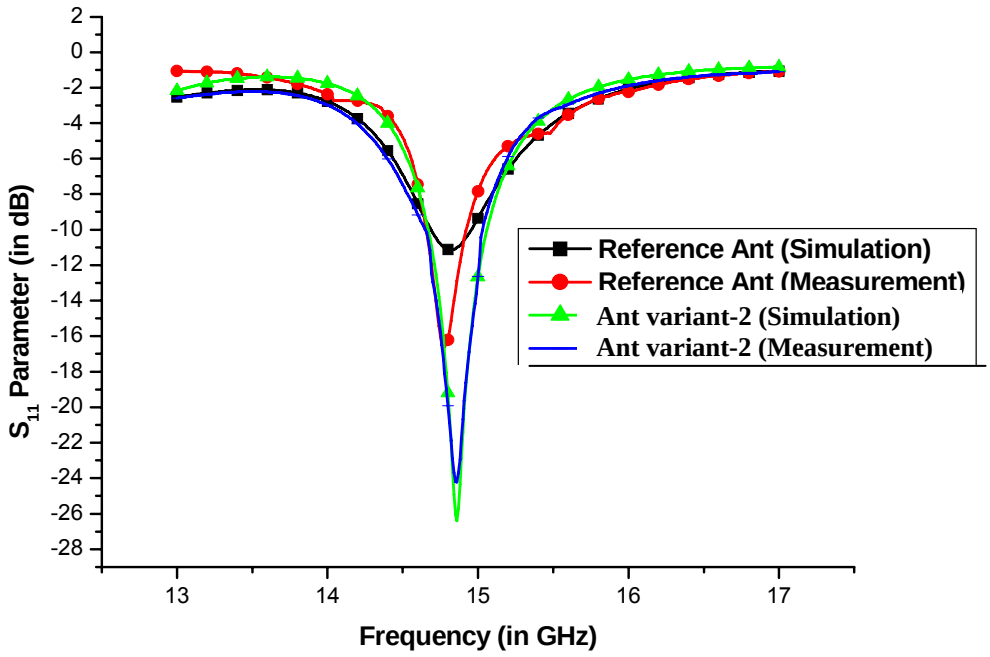

Fig. 4.6 S_{11} parameter Vs frequency graph obtained from measurement for reference antenna and antenna variant-2 having EBG pattern-2

The simulated and measured S_{11} parameter values at central frequency of 14.8 GHz for reference antenna and antenna variant-2 are tabulated in Table 4.6.

Table 4.6: S_{11} parameter results for reference antenna and antenna variant-2 obtained from simulation and measurement at central frequency of 14.8 GHz

	Simulation Result	Measurement Result
Reference Antenna	-11.15 dB	-16.5 dB
Antenna variant-2	-26.38 dB	-24.1 dB

From Table 4.6 we observe that the simulated and measured S_{11} parameter results for reference antenna and antenna variant-2 are in agreement with each other. The S_{11} parameter value for antenna variant-2 is higher in comparison to the reference antenna. This means that as we etch the feedline with the EBG structure, we get a better S_{11} parameter.

4.3.2.2 Bandwidth

The bandwidth of the reference antenna and antenna variant-2 is found from simulation and measurement. Both simulation and measurement results are found to be in agreement with each other. The bandwidth values of the antennas have been tabulated in Table 4.7.

Table 4.7: Bandwidth results for reference antenna and antenna variant-2 obtained from simulation and measurement at central frequency of 14.8 GHz

	Simulation Result	Measurement Result
Reference Antenna	0.2682 GHz	0.256 GHz
Antenna Variant-2	0.3912 GHz	0.3712 GHz

From Table 4.7, we observe that by etching EBG patterns on the feedline we can improve the bandwidth of antenna variant-2 by upto 45% when compared with the

reference or the prototype antenna. The EBG pattern is shown in Fig. 3.7 in Chapter 3. Hence, a considerable improvement in bandwidth is obtained.

4.3.2.3 Current Distribution

The current distribution graph for antenna variant-2 is obtained and shown in Fig. 4.7.

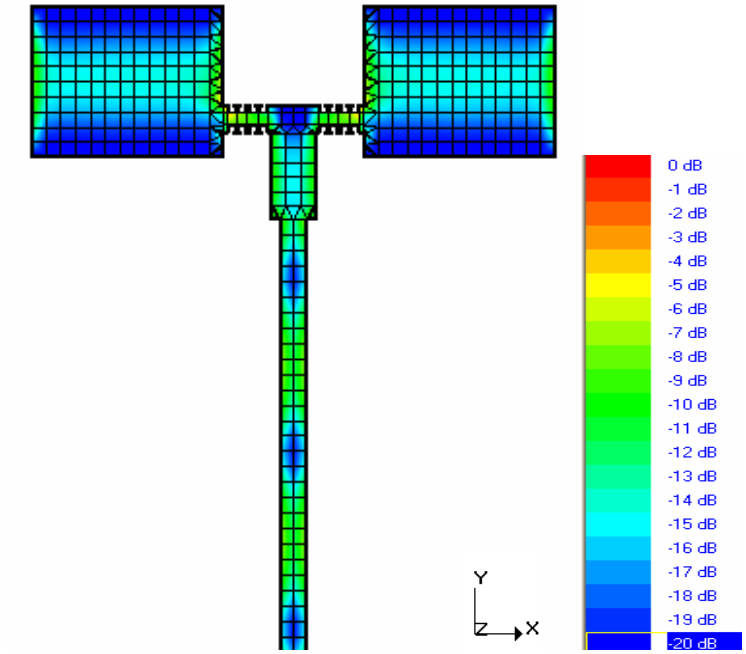

Fig. 4.7 Current distribution for antenna variant-2

From Fig. 4.7, we see that at and near the dummy EBG patterns the magnitude of current distribution is minimized when compared to the current distribution for reference antenna shown in Fig. 4.3(a) due to a change in the antenna impedance. Change in current distribution leads to a change in antenna performance parameters as shown in Table 4.8.

4.3.2.4 Radiation Patterns

The radiation pattern for antenna variant-2 is obtained from measurement and is shown in Fig. 4.8. Both *E*-plane and *H*-plane are shown. Also, cross polarization is shown.

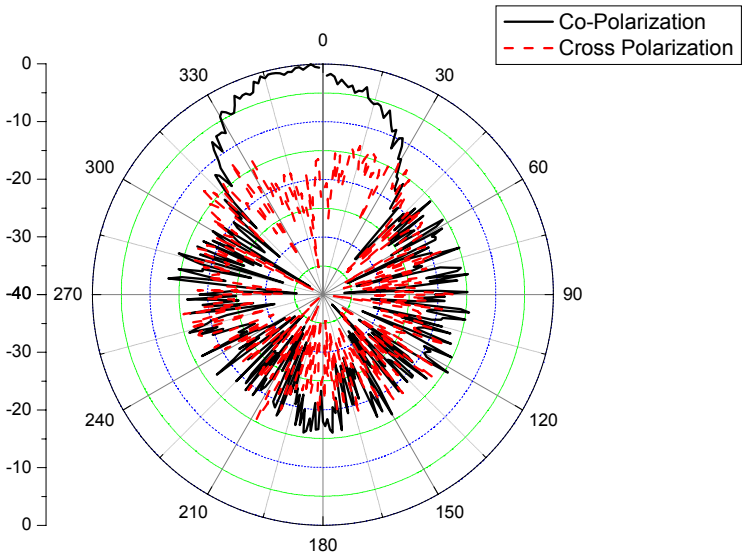

(a) *E* Plane

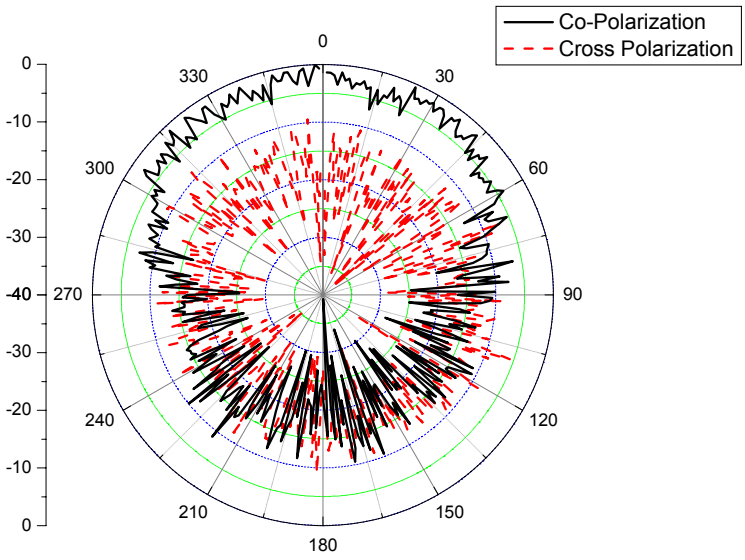

(b) *H* Plane

Fig. 4.8 Radiation patterns for antenna variant-2 measured at 14.8 GHz

From Fig. 4.8(a) we observe that the respective *E*-plane radiation pattern for antenna variant-2 is similar to the *E*-plane radiation pattern obtained for reference antenna shown in Fig. 4.4(a). Similarly, the respective *H*-plane pattern for antenna variant-2 is similar to the *H*-plane pattern for reference antenna shown in Fig. 4.4(b). Both *E* plane and *H* plane radiation patterns do not change significantly. This is an expected result.

Due to the limitation of the measuring chamber, we experience a large noise in the measurement results.

4.3.2.5 Other Antenna Parameters

Table 4.8 tabulates radiation efficiency, antenna efficiency and linear gain for the reference antenna and antenna variant-2.

Table 4.8: Other important antenna parameters for reference antenna and antenna variant-2 at central frequency of 14.8 GHz

Antenna Performance	Reference Antenna	Antenna variant-2
Radiation Efficiency	88.58%	88.91%
Antenna Efficiency	81.71%	86.83%
Linear Gain	9.71 dBi	9.94 dBi

It is observed from Table 4.8 that the antenna efficiency and linear gain for antenna variant-2, i.e., antenna having EBG pattern-2 is improved when compared to the reference antenna. Thus, the EBG pattern etched on the feedline helps us to give a greater bandwidth and at the same time improves the efficiency and the gain of the antenna.

4.3.3 Antenna Variant-3 Vs Reference Antenna

Similar to the previous two Sections 4.3.1 and 4.3.2, in this section, we will compare measurement results of antenna variant-3 with reference antenna. The feedline position for antenna variant-3 is fixed at a distance of 1.0 mm measured from bottom of twin patches. Fabricated antenna variant-3 used for obtaining measurement results has been shown in Fig. 3.8 in Chapter 3.

4.3.3.1 S_{11} Parameters

The S_{11} parameter value Vs frequency in GHz graph for the reference antenna and antenna variant-3 is obtained by simulation and measurement and is shown in Fig. 4.9.

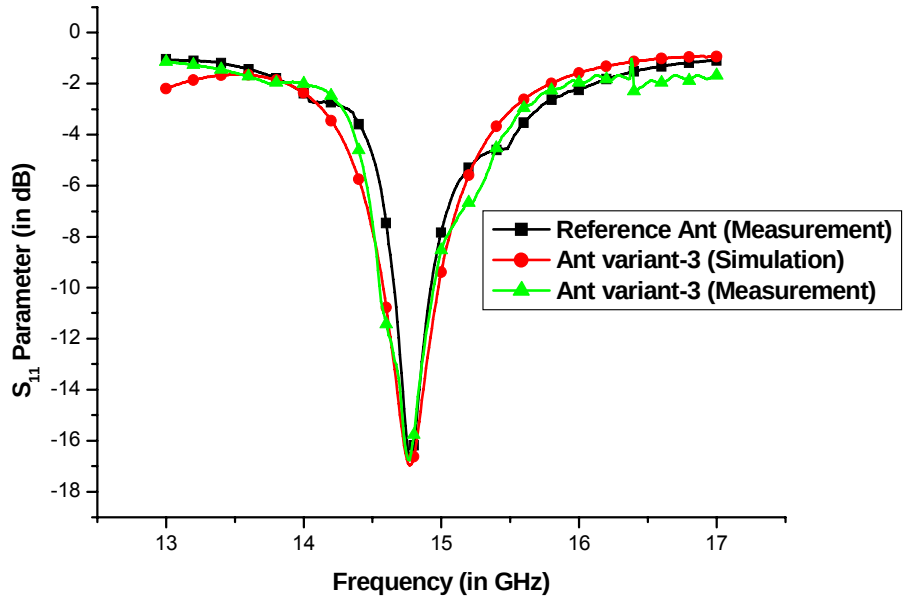

Fig. 4.9 S_{11} parameter Vs frequency graph obtained from measurement for reference antenna and antenna variant-3 having EBG pattern-3

The simulated and measured S_{11} parameter values for reference antenna and antenna variant-3 are tabulated in Table 4.9.

Table 4.9: S_{11} parameter results for reference antenna and antenna variant-3 obtained from simulation and measurement at central frequency of 14.8 GHz

	Simulation Result	Measurement Result
Reference Antenna	-11.15 dB	-16.5 dB
Antenna variant-3	-16.97 dB	-17 dB

From Table 4.9 we observe that the simulated and measured results of S_{11} Parameter for reference antenna and antenna variant-3 are in agreement with each other. The S_{11} parameter values obtained are greater than -10 dB in the passband range which is a desirable result. Also, the S_{11} parameter value for antenna variant-3 is higher in comparison to the reference antenna.

4.3.3.2 Bandwidth

The bandwidths of the reference antenna and antenna variant-3 are obtained from simulation and measurement. Both simulation and measurement results are found to be in agreement with each other. The bandwidth values of the antennas have been tabulated in Table 4.10.

Table 4.10: Bandwidth results for reference antenna and antenna variant-3 obtained from simulation and measurement at central frequency of 14.8 GHz

	Simulation Result	Measurement Result
Reference Antenna	0.2682 GHz	0.256 GHz
Antenna Variant-3	0.4005 GHz	0.3928 GHz

From Table 4.10, we observe that the by etching EBG patterns on the feedline, we can improve the bandwidth of antenna variant-3 by upto 53.4 % when compared with the reference or the prototype antenna. The EBG pattern has been shown in Fig. 3.10 in Chapter 3.

4.3.3.3 Current Distribution

The current distribution graph for antenna variant-3 is shown in Fig. 4.10.

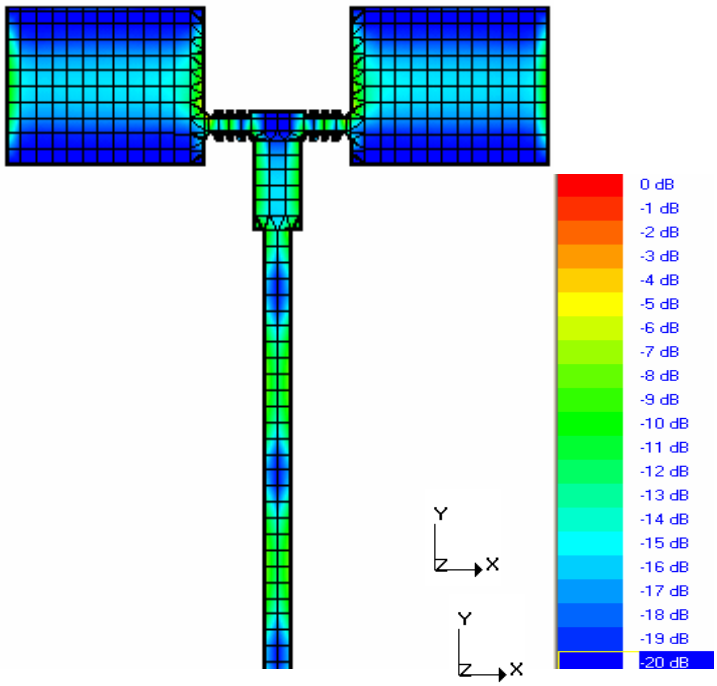

Fig. 4.10 Current distribution for antenna variant-3

From Fig. 4.10, we see that at and near the dummy EBG patterns the magnitude of current distribution is minimized for antenna variant-3 due to a change in the antenna impedance after etching the EBG structures. As a result, the antenna performance parameters are changed and this has been shown in Table 4.11.

4.3.3.4 Radiation Patterns

The radiation pattern for antenna variant-3 is obtained from measurement and is shown in Fig. 4.11. Both *E*-plane and *H*-plane are shown in the figure.

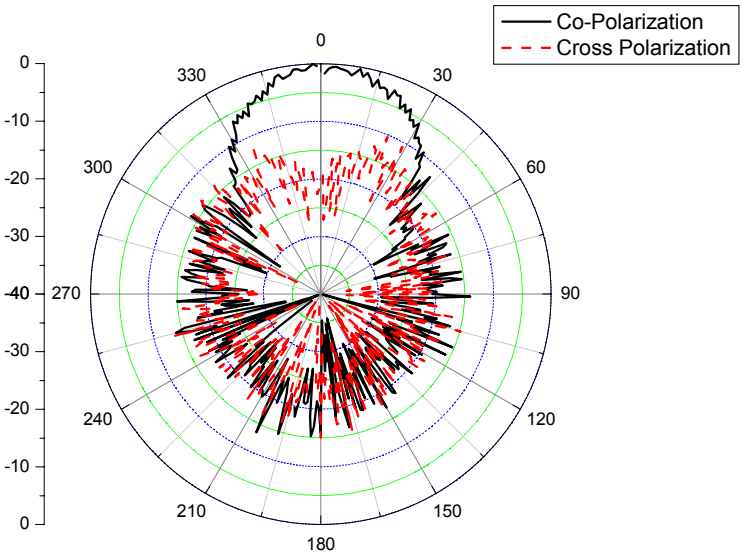

(a) *E* Plane

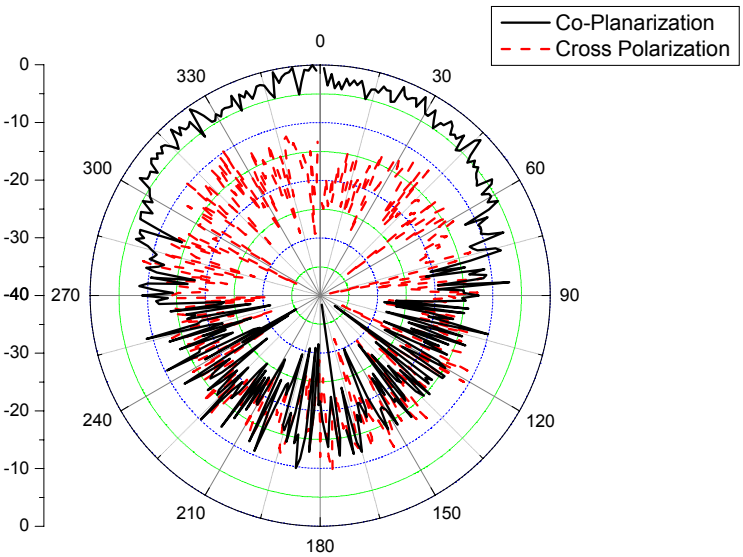

(b) *H* Plane

Fig. 4.11 Radiation patterns for antenna variant-3 measured at 14.8 GHz

Similar to the results obtained in Sections 4.3.1.4 and 4.3.2.4, the respective *E*-plane and *H*-plane radiation patterns for reference antenna and antenna variant-3 do not significantly change.

Also, due to the limitation of the measuring chamber, a significant noise is observed in the measurement results and hence we are not able to obtain a smooth curve.

4.3.3.5 Other Antenna Parameters

Table 4.11 tabulates radiation efficiency, antenna efficiency and linear gain for reference antenna and antenna variant-3.

Table 4.11: Other important antenna parameters for reference antenna and antenna variant-3 at central frequency of 14.8 GHz

Antenna Performance	Reference Antenna	Antenna variant-3
Radiation Efficiency	88.58%	88.72%
Antenna Efficiency	81.71%	85.96%
Linear Gain	9.71 dBi	9.89 dBi

It is observed from Table 4.11 that the antenna efficiency and linear gain for antenna variant-3, i.e., antenna having EBG pattern-3, is improved when compared to the reference antenna.

4.4 Summary

In this Chapter, we investigated the significance of the feedline position with respect to the bandwidth improvement. It was shown that the best position of the feedline to have the maximum improvement in bandwidth for our antenna design should be

closer to the lower edge of the twin patches. Bandwidth results of reference antenna were compared to its three variants and a significant improvement in bandwidth was shown.

Bandwidth of antenna having EBG pattern-1, EBG pattern-2 and EBG pattern-3 is shown to be improved by 48 %, 45 % and 53.4 %, respectively when compared to the reference antenna. Other antenna parameters such as antenna efficiency and gain are shown to be improved.

CHAPTER 5

CONCLUSION

5.1 Summary

Patch antennas are very popular because of their low profile nature, light weight and low costs. They have many advantages over conventional antennas. However, narrow bandwidth is a major problem.

In this thesis, the narrow bandwidth problem of a dual patch microstrip antenna was studied. The method employed to improve its bandwidth is etching the feedline connecting the twin patches by patterns that are similar in nature. These patterns are not etched on the ground plane; however these patterns resemble in their properties and behavior to conventional EBG structures and hence have been termed as dummy EBG patterns.

Three different EBG patterns are proposed and measurement results confirm that antennas having EBG patterns etched on the feedline have considerable improvement in bandwidth when compared to a reference antenna having no EBG pattern etched. These EBG patterns have been termed according to their physical shape and geometry, viz., Opposite Double-E EBG pattern, Top Hat dummy EBG pattern, and Hut-shaped EBG pattern.

Also, the significance of the position of feedline connecting the twin patches is explored and studied by shifting the feedline to different positions ranging from the lower edge towards the upper edge of the patch. It is found that antenna with feedline

closer to the lower edge of the patch has a higher bandwidth when compared to antenna with feedline closer to the upper edge. Also, antennas having EBG patterns etched on the feedline have a considerably higher bandwidth value when compared to the reference antenna for the same feedline position. However, sensitivity of bandwidth to change in position of feedline with EBG pattern etched is reduced. Hence, we get a much higher percentage improvement in bandwidth for antenna with EBG pattern etched on the feedline when compared to a reference antenna when the feedline is closer to the lower edge.

5.2 Important Results

Firstly, we compare the bandwidths of reference antenna and antenna with feedline having EBG pattern etched by changing the position of the feedline to different locations. It is found that the best increment in bandwidth is obtained when the feedline position is closer to the lower edge of the patch. This distance is found to be 1.0 mm measured from the bottom of the twin patches for our antenna design.

Bandwidth of the reference antenna is found to be 0.256 GHz by measurement when the feedline is at a distance of 1.0 mm measured from the bottom of the twin patch. Bandwidth of antennas having different EBG patterns etched on the feedline, namely, Double-E EBG pattern, Top Hat dummy EBG pattern, and Hut-shaped EBG pattern have a bandwidth value of 0.381 GHz, 0.3712 GHz, and 0.3928 GHz, respectively obtained by measurement. Thus, the percentage improvement in bandwidth is about 48%, 45% and 53.4%, respectively, for antennas with EBG patterns when compared to the reference antenna.

Other antenna parameters are also obtained. Antenna efficiency and gain of the antennas with EBG patterns etched on the feedline is improved when compared to the reference antenna. Radiation efficiency and radiation patterns remain almost the same for all the antennas. This was expected because radiation is due to the patches which remain the same in all the structures.

5.3 Future Work

In this thesis, we examined a dual array rectangular patch antenna and the use of EBG structure on the feedline to help improve the bandwidth. The future work can involve changing the antenna type (including antenna shape and the dielectric of the substrate) and carry out further research into the EBG structures.

Besides, we can also use different shapes of microstrip patches such as square shape and circular shape patch to carry out the research. While examining, similar EBG patterns proposed in the thesis can be etched on the feedline of the proposed new antennas. Hence, one can formulate the results for every kind of patch shape for a patch antenna.

Another area where one can further research on is by changing the shape of EBG patterns etched on the feedline. Thus, by keeping the rectangular patch, other shape and size of EBG patterns can be examined and new results can be obtained.

REFERENCES

[1] Balanis, C.A., Antenna Theory: Analysis and Design, John Wiley & Sons, Inc, 1997.

[2] E. Yablonvitch, "Photonic band-gap structures," J. Opt. Soc. Amer. B, Opt. Phys. , vol. 10, no. 2, pp. 283-295, Feb 1993.

[3] Fan Yang and Rahmat–Samii, Y, "Applications of electromagnetic band-gap (EBG) structures in microwave antenna designs," Microwave and Millimeter Wave Technology, pp. 528-531, Aug 2002.

[4] Shakelford, A., Lee, K.F., Luk, K.M.," Design of small-size wide-bandwidth microstrip patch antennas," Antennas and Propagation Magazine, IEEE, vol. 45, Issue 1, pp. 75-83, Feb. 2003.

[5] Ting-Hua Liu and Wen Xun Zhang, "Compound techniques for broadening the bandwidth of microstrip patch antenna," Microwave Conference Proceedings, vol. 1, pp. 241-244, Dec. 1997.

[6] Adilena Slavova, A. Abdel Rahman and A.S. Omar, "Broadband bandwidth enhancement of an Aperture coupled microstrip patch antenna," Antennas and Propagation Society International Symposium, vol. 4, pp. 3737-3740, June 2004.

[7] Tao Yuan, Jian-Ying Li, Le-Wei Li, Lei Zhang, and Mook-Seng Leong, "Improvement of Microstrip Antenna Performance Using Two Triangular Structures", Digest of 2005 IEEE Antennas and Propagation Society International Symposium, vol. 1A, pp. 301-304, 3-8 July 2005.

[8] J.Y. Li, Zaw-Zaw Oo, and Le-Wei Li, "Improvement of characteristics of microstrip antennas using unbalanced structures," IEEE Antennas and wireless Propagat. Lett, vol. 1, pp. 71-73, 2002.

[9] Kumar, G. and Ray, K.P., Broadband Microstrip Antennas, Artech House, Inc, 2003.

[10] Garg, R., Bhartia, P., Bahl, I., Ittipiboon, A., Microstrip Antenna Design Handbook, Artech House, Inc, 2001.

[11] Qian Y., Coccioli R., Sievenpiper D., Radisic V., Yablonovitch E., and Itoh T., "A Microstrip Patch Antenna using novel photonic bandgap structures", Microwave J., vol 42, pp. 66-76, Jan 1999.

[12] Stutzman, W.L. and Thiele, G.A., Antenna Theory and Design, John Wiley & Sons, Inc, 1998.

[13] Balanis, C.A., Advanced Engineering Electromagnetics, John Wiley & Sons, New York, 1989.

[14] Hammerstad, E.O., "Equations for Microstrip Circuit Design," Proc. Fifth European Microwave Conf., pp. 268-272, September 1975.

[15] James, J.R. and Hall, P.S., Handbook of Microstrip Antennas, Vols 1 and 2, Peter Peregrinus, London, UK, 1989.

[16] Bahl, I.J. and Bhartia, P., Microstrip Antennas, Artech House, Dedham, MA, 1980.

[17] Richards, W.F., Microstrip Antennas, Chapter 10 in Antenna Handbook: Theory Applications and Design (Y.T. Lo and S.W. Lee, eds.), Van Nostrand Reinhold Co., New York, 1988.

[18] Newmanm E.H. and Tylyathan, P., "Analysis of Microstrip Antennas Using Moment Methods," IEEE Trans. Antennas Propag., vol. AP-29, No. 1, pp. 47-53, January 1981.

[19] Harrington. R.F., Field Computation by Moment Methods, Macmillan, New York, 1968.

[20] Kantorovich, L. and Akilov, G., Functional Analysis in Normed Spaces, Pergamon, Oxford, pp. 586-587, 1964.

[21] E.R. Brown, C.D. Parker, and E.Yablonovitch, "Radiation properties of a planar antenna on a photonic-crystal substrate," J. Opt. Soc. Am. B., vol. 10, pp.404-407, Feb 1993.

[22] M. Thevenot, M.S. Denis, A.Reincix, and B. Jecko, "Design of a new photonoic cover to increase antenna directivity," Microwave Opt. Technol. Lett, vol. 22, no. 2, pp. 136-139, July 1999.

[23] D. Sievenpiper, L. Zhang, R.F. J. Broas, N. G. Alexopolous, and E. Yablonovitch, "High-impedance electromagnetic surfaces with a forbidden frequency band," IEEE Trans. Microw. Theory Tech., vol. 47, no. 11, pp. 2059-2074, Nov. 1999.

[24] L. Yang, M.Y. Fan, F.L. Chen, J.Z. She, and Z.H. Feng, “A novel compact Electromagnetic Bandgap structure and its applications for microwave circuits,” in IEEE Trans. Microwave Theory and Techniques, vol. 53, no. 1, pp. 183-190, Jan 2005.

[25] Ang Yu, Xuexia Zhang, “A novel 2-D electromagnetic band-gap structure and its application in micro-strip antenna arrays,” Microwave and Millimeter Wave Technology, pp. 580-583, Aug 2002.

[26] Li Yang, Mingyan Fan, and Zhenghe Feng, “A Spiral Electromagnetic Bandgap (EBG) Structure and its Application in Microstrip Antenna Arrays,” IEEE APMC, vol. 3, 4pp., Dec 2005.

[27] Xu Daoxian, Ooi Ban Leong, and Zhao Guang, “A New Triple-band Slot Antenna with EBG Feed,” Proceeding of Microwave, Antenna, Propagation and EMC Technologies for Wireless Communication, vol. 1, pp. 41-44, Aug 2005.

[28] Vesna Radisic, Yongxi Qian, Roberto Coccioli and Tatsuo Itoh, “Novel 2-D Photonic Bandgap Structure for Microstrip Lines”, IEEE Microwave and Guided Wave Letter, Vol. 8, pp. 69-71, 1998.

[29] IE3D 11.0, Zeland Software Inc., Fremont, CA.